Evolutionary morphology of the coelurosaurian arctometatarsus: descriptive, morphometric and phylogenetic approaches

ERIC SNIVELY*, ANTHONY P. RUSSELL FLS and G. LAWRENCE POWELL

Vertebrate Morphology Research Group, Department of Biological Sciences, The University of Calgary, 2500 University Dr. NW, Calgary, Alberta T2N 1N4, Canada

Descriptive, principal component (PCA), and thin-plate spline (TPS) analyses of theropod third metatarsals (MT III) definitively segregate the arctometatarsus from other theropod pedal morphologies and reveal variation within phylogenetic and functional subgroups of metatarsi. PCA indicates that the arctometatarsalian MT III differs in shape from the nonarctometatarsalian condition independently of size, indicating that allometric differences among taxa produced this divergence in MT III shape. TPS indicates substantial transfer of footfall force from MT II to MT III in ornithomimids and tyrannosaurids and from MT IV to MT III in troodontids. The study suggests different modes of ligament-damped sagittal rotation of MT III in tyrannosaurids, ornithomimids, and troodontids. *Deinonychus* had a large MT II–MT III articulation consistent with resisting forces of predatory strikes, while MT III of some large carnosaurs are less robust than expected. Phylogenetic bracketing suggests that proximal intermetatarsal ligaments in theropods were a key innovation preceding arctometatarsus evolution. A Bayesian phylogenetic analysis indicates that an arctometatarsus evolved in the common ancestor of the Tyrannosauridae + (Ornithomimosauria + Troodontidae) clade, but other optimizations are plausible. The most likely selective benefit of the structure was increased agility; if so, homoplasy indicates multiple exaptive and adaptive pathways towards predation and escape roles. © 2004 The Linnean Society of London, *Zoological Journal of the Linnean Society*, 2004, **142**, 525–553.

ADDITIONAL KEYWORDS: evolution – metatarsus – principal component analysis – selection – Theropoda – Tyrannosauridae.

INTRODUCTION

During the Cretaceous an unusual foot morphology, the arctometatarsus (Holtz, 1995), evolved several times amongst coelurosaurian theropod dinosaurs. Major phylogenetic hypotheses of coelurosaurian relationships differ in their optimization of this morphology and lead to different inferences about its evolution (Fig. 1). Holtz (1995) incorporated four characteristics into the osteological definition of the arctometatarsus:

1. the third (central) metatarsal (MT III) is constricted proximally relative to the condition in other theropods;

2. MT III is also triangular in distal transverse cross section and thus constricted towards the plantar surface;

3. the outer, weight-bearing metatarsals, the second and fourth (MT II and IV), encroach towards the midsagittal plane of MT III where it is constricted, and

4. maintain contact with MT III distally and proximally. All three metatarsals therefore form a wedge-and-buttress morphology, in which buttressing surfaces of the outer metatarsals overhang and contact distal surfaces of the wedgelike third metatarsal (Holtz, 1995).

Variants of the arctometatarsus evolved in Asian alvarezsaurids (Perle *et al.*, 1994; Karhu & Rautian, 1996; Chiappe, Norell & Clark, 2002), which lack a proximal splint of MT III, and in the enigmatic *Avimimus por-*

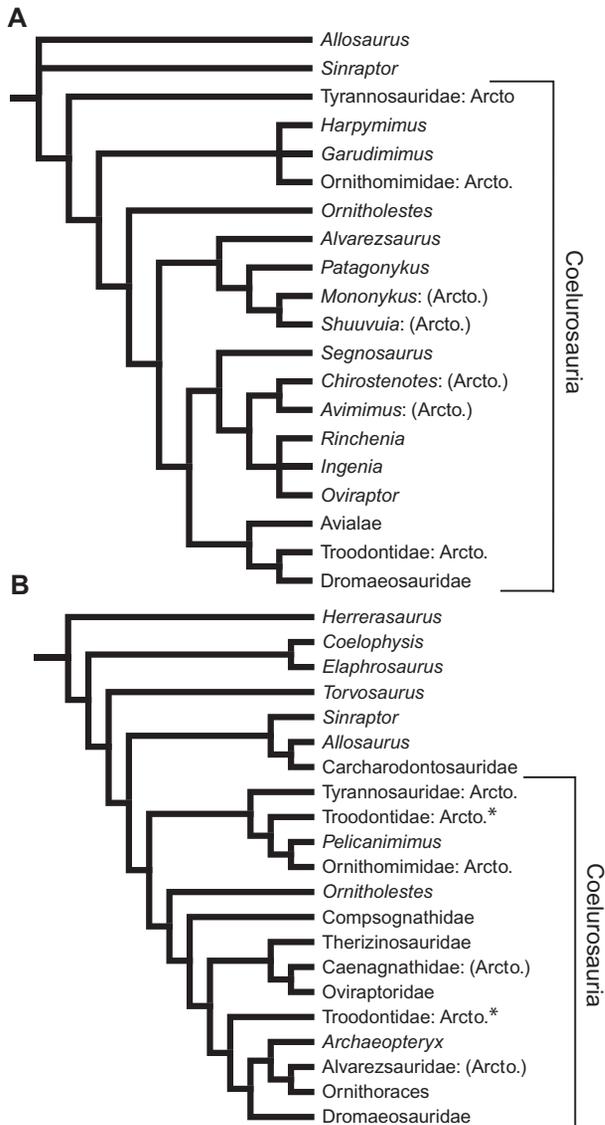*Corresponding author. E-mail: esnively@ucalgary.ca

Figure 1. Phylogenetic hypotheses of coelurosaurian relationships: (A) after Clark *et al.* (2002), and (B) after Holtz (2000). The designation 'Arcto.' signifies the occurrence of an arctometatarsus, with a proximal splint of metatarsal III (MT III) that is unfused to MT II and MT IV and a triangular distal cross section (Holtz, 1995). The designation '(Arcto.)' indicates a variant on this morphology, with proximal fusion of MT II–IV (the caenagnathid *Elmisaurus*), gradual tapering of MT III proximally rather than a rectangular splint (the caenagnathid *Chirostenotes*), or the loss of the proximal portion of MT III (Asian alvarezsaurids such as *Mononykus* and *Parvicursor*). (B) shows the arctometatarsus as a synapomorphy of an ornithomosaur–tyrannosaurid clade. *Signifies alternate placements of Troodontidae.

tenosus, in which the proximally constricted region is not preserved (Kurzanov, 1983).

In addition to its osteological characteristics, several authors have commented on the likely presence of ligaments that bound the arctometatarsus together. Snively & Russell (2002, 2003) reported rugosities on closely adjoining articular surfaces of tyrannosaurid metatarsals and presented evidence that the rugosities represent ligament scars. Rugosity is especially prominent on the distal wedge and buttress surfaces of MT II and III. Holtz (1995) and Hutchinson & Padian (1997) noted that such ligaments would have provided strong articulation of the metatarsals. This indicates for the alvarezsaurids that distal intermetatarsal ligaments were the only mechanism of articulation between the distally restricted MT III and the outer elements.

The ligaments and bones of the arctometatarsus have been hypothesized as a complex, low displacement elastic system (Coombs, 1978; Wilson & Currie, 1985; Holtz, 1995; Snively & Russell, 2003). Transfer of footfall energy from MT III to adjoining elements may have been the most broadly distributed function (Wilson & Currie, 1985; Holtz, 1995; Snively, 2000). Slight posterior rotation of the proximal splint of MT III may have been possible in some forms (Wilson & Currie, 1985), especially troodontids. Longitudinal pistoning of the third metatarsal (Coombs, 1978) was possible over very short excursions (Holtz, 1995) but probably could not aid forward progression (Snively, 2000). In tyrannosaurids, ligaments and the triangular distal cross section of MT III are hypothesized to have acted to passively unify the foot under high loadings (Snively & Russell, 2002, 2003).

Evaluating these hypotheses demands parsing of morphological variation between arctometatarsalian forms. Holtz (1995) concisely describes the entire metatarsus of theropods. Because the third metatarsal affected the development and function of adjacent load-bearing elements, it occupies a central role anatomically and analytically. Classifying MT III specimens by form rather than phylogeny allows us to deduce functional similarities, regardless of ancestry, and to assess adaptation and convergence. A thorough assessment of theropod MT III diversity is necessary to place the arctometatarsus into systematic and functional frameworks and to consider its roles in theropod evolution. Both descriptive and mathematical techniques are useful for addressing these issues.

Description is a salutary prerequisite to mathematical inquiries into morphological diversity. While quantitative analysis is ostensibly a more objective starting point, grounding in qualitative data is necessary for assessing previous morphological perceptions (Grande & Bemis, 1998) and for interpreting statistical results (Pimentel, 1979). Statistical methods must

yield wholly to morphological description when sample size is very low (often the case with palaeontological specimens; Kemp, 1999). However, with an adequate sample, multivariate statistics can both quantify and augment descriptive analyses of variation.

Principal component analysis (PCA) is a useful method for quantifying morphometric variation. It distils trends in voluminous suites of measurements by identifying major aspects of variation and covariation in size and shape. PCA clusters objects by interrelationships of absolute size and relative proportions, and can therefore test whether size effects statistically (and perhaps mechanically) overwhelm ostensible similarities in shape. MT III of juvenile ornithomimids and the largest tyrannosaurids are qualitatively classifiable as arctometatarsalian, but their body masses span over three orders of magnitude (Paul, 1988; Henderson, 1999). With this large size range, a quantitative check of apparent morphological similarity allows more rigorous constraint on functional hypotheses. (Appendix 1 explains our rationale and approach for applying PCA to palaeontological data.)

If PCA shows significant clustering by shape regardless of size, morphometrics that emphasizes proportional differences can further test ideas of shape and functional variation. Thin-plate spline analysis (TPS) reveals the degree of deformation necessary to mathematically transform one shape into another (Bookstein, 1991). Outlines of two objects are decomposed into coordinates for landmarks, which can represent homologous points and proportional distances. Two landmarks are chosen as reference points to normalize the objects for size. TPS calculates Procrustes distances (independent of a coordinate baseline) between corresponding points on two objects, and thus quantifies the magnitude and direction (partial warp scores) of 'warping' between equivalent landmarks. The warping can be affine (analogous to tilting of a rigid plate), or nonaffine, based on the 'bending energy' necessary to deform a plate. TPS is useful for characterizing subtleties and continua of variation that are difficult to describe, and with appropriate landmark choice can test hypotheses of three dimensional variation (Swiderski, 1994; Ahlström, 1996) and functional evolution (Jasinoski, 2003). For example, TPS can help answer questions about functional variation in slightly differing arctometatarsalian morphologies, if it incorporates points corresponding to mechanically salient features.

Quantified and described variation in theropod third metatarsals can elicit hypotheses of immediate function, which would have played roles in locomotion and food procurement. This study employs descriptive and morphometric methods to test three hypotheses of theropod MT III variation. (Ha): metatarsi classified as arctometatarsalian (Holtz, 1994, 1995), regardless of size, share a significantly greater degree of proximal MT III constriction than do those of other theropods. (Hb): arctometatarsalian MT III are phylogenetically differentiable in their degree of relative proximal constriction, in accordance with the hypotheses of relationship in Figure 1. (Hc): tyrannosaurids, troodontids, and ornithomimids differed in modes of footfall energy transmission.

In order to evaluate hypotheses of variation in an evolutionary context, we conduct Bayesian inference analyses on two theropod data matrices, and optimize the morphology onto the resulting trees. Analysis of the matrix of Holtz (2000) tests the likelihood of several equally optimal trees. This taxonomically broad data set tests the distribution of characters relevant to arctometatarsus evolution throughout Theropoda. Analysis of data from Clark, Norell & Makovicky (2002) applies Bayesian inference to a matrix that does not collapse terminal taxa, and facilitates more precise optimization of the arctometatarsus within Coelurosauria. With results yielding reciprocal perspectives on variation and phylogeny, we then discuss arctometatarsal evolution in light of its bone and ligament morphology, hypothesized mechanical function, and possible biological role (selective benefit).

Institutional abbreviations

AMNH	American Museum of Natural History, New York
BYU	Brigham Young University, Provo
DINO	Dinosaur National Monument, Jensen
FIP	Florida Institute of Palaeontology, Dania Beach
FMNH	Field Museum of Natural History, Chicago
FPMN	Fukui Prefectural Museum of Nature, Japan
GI	Geological Institute, People's Republic of Mongolia, Ulan Bator
IVPP	Institute of Vertebrate Palaeontology and Palaeoanthropology, Beijing
MOR	Museum of the Rockies, Bozeman
NAMAL	North American Museum of Ancient Life, Lehi
NMC	Canadian Museum of Nature, Aylmer
PIN	Palaeontological Institute of the Russian Academy of Sciences, Moscow
PVPH	Palaeontologia de Vertebrados, Museo de Neuquén
ROM	Royal Ontario Museum, Toronto
TMP	Royal Tyrrell Museum of Palaeontology, Drumheller
TMP/PJC	Photograph or TMP specimen in care of P.J. Currie

UCMP   University of California Museum of Palaeontology, Berkeley

UCMZ(VP) University of Calgary Museum of Zoology, Vertebrate Palaeontology Collection, Calgary

YPM   Yale Peabody Museum, New Haven.

MATERIAL AND METHODS

DATA COLLECTION

For the morphological descriptions we follow the conventions of Holtz (1995). We refer to cross section as a plane perpendicular to the metatarsal long axis, and anterior view as that of the dorsiflexed surface of the metatarsal when it is perpendicular to the substrate. (Anterior in the metatarsus of the standing animal corresponds to dorsal in the early development of the limb.) We equate plantar with posterior in reference to the metatarsus (Fig. 2A).

Appendix 2 and Figures 3–9 document specimens examined for description and measured for PCA according to the template (Fig. 2B) showing landmarks and measured distances between them. Using Mitutoyo digital calipers and tape measure for distances greater than 60 cm, we averaged three measurements for overall length (LTOTAL), distal and proximal widths (WDIST and WPROX), three evenly spaced transverse widths (W25%, W50%, W75%), and the height (proximodistal extent) of the phalangeal articular surface in anterior view (HPAS).

Measurements of *Ingenia yanshini* and *Rinchenia mongoliensis* specimens (Fig. 9) were taken from slides of original specimens photographed by P. J. Currie and scaled to his measurements of overall MT III length. Accuracy of such measurements was assessed
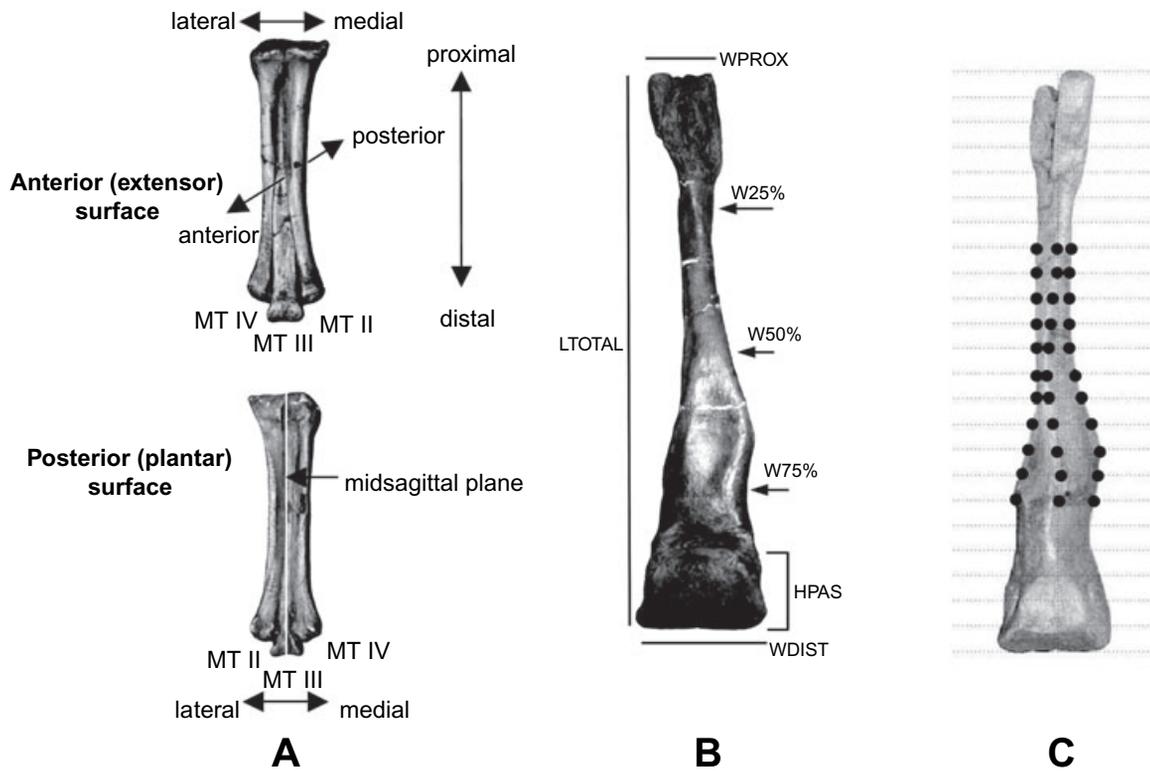

Figure 2. Descriptive conventions and morphometric templates for examining theropod third metatarsal (MT III) variation. A, directional and positional adjectives used in the descriptions, diagrammed on anterior (top) and posterior (bottom) views of an *Elmisaurus* sp. metatarsus. B, measurements for principal component analysis (PCA), diagrammed on anterior view of *Tyrannosaurus rex* MT III: LTOTAL, total length; WPROX, proximal width; W25%, width at 25% of TL from proximal end. W50%, width at 50% of TL; W75%, width at 75% of TL from proximal end; WDIST, distal width; HPAS, proximodistal extent (height) of phalangeal articular surface in anterior view. C, landmarks for thin-plate spline analysis, represented as dots on a posterior view of a *T. rex* MT III. Points represent the lateral and medial anterior edges of the metatarsus, and the apex of the plantar constriction, at 11 cross sections along the shaft. The number of cross sections best encompassed the region of plantar constriction for all three taxa, starting with the distalmost cross section through the region.

by comparing physical and scale-bar normalized measurements from photographs of other specimens. The accuracy was within ± 2%, and proportions remained consistent from specimen to photograph.

Photographs for the thin-plate spline analyses were taken with the specimen's anterior surface parallel to the plane of the camera lens, with no apparent angular distortion. Specimens were positioned with clay and sandbags. The orientation was double checked by running TPS with later photographs of several specimens; differences in partial warp scores were nonexistent to negligible.

PRINCIPAL COMPONENT ANALYSIS

Appendix 2 lists absolute measurements for all specimens. PCA was performed in SYSTAT on $\log_{10}$-transformed measurements. PCI represents variation associated with absolute size (Pimentel, 1979). We were interested in determining aspects of shape variation that are independent of absolute size (such as those influenced by general allometric scaling). We therefore ran a second PCA upon a data set derived from the original data, but manipulated statistically such that the influence of geometric similarity (or isometry) was removed (Burnaby, 1966). The results of this PCA would aid in identifying the influences of allometry and nonsize-associated variance upon MT III of different sizes. Appendix 1 elaborates on the details and reasoning behind these methods.

THIN-PLATE SPLINE ANALYSIS

To examine differences in plantar constriction in ornithomimid, tyrannosaurid, and troodontid specimens, TPS was run on coordinates digitized from photographs in posterior view (Fig. 2C). Landmark coordinates were determined from scanned photographs, in which all specimens were normalized to 600 pixels in height. Using MakeFan software, posterior metatarsal images were longitudinally divided by 24 lines and bisected by one line along the long axis of MT III. With the assistance of these lines, landmark coordinates along the region of the plantar constriction were digitized using TPSdig software. These semi-landmarks (positionally if not developmentally corresponding) began at the base of the plantar constriction, and included 11 evenly spaced points each along the lateral and medial edges of MT III, and 11 points along the plantar midline of MT III or along the ridge of the constriction where it deviates from the midline.

TPSspline calculated and provided vector images of partial warp scores, showing Procrustes-normalized displacements between corresponding landmarks in different metatarsal images.

BAYESIAN INFERENCE ESTIMATION OF THEROPOD PHYLOGENY

Holtz's (2000, 2001) phylogenetic analyses yielded equally parsimonious trees in which Troodontidae was alternately sister to Ornithomimosauria or to dromaeosaurs + birds. To independently determine which hypothesis was more robust, and to assess the hypotheses with a separate data set, we applied Bayesian inference analyses (Huelsenbeck *et al.*, 2001) to the data matrices of Holtz (2000) and of Clark *et al.* (2002). Bayesian inference tests the probability that a clade is correct given the data, with lower branch lengths correlating with higher probabilities (Felsenstein, 1981; Bergmann, 2003). As currently implemented, the method arrives at final posterior probability values for clades via a Markov chain Monte Carlo (MCMC) approach (Green, 1995; Larget & Simon, 1999; Mau, Newton & Larget, 1999). A tree is randomly perturbed, and the original or perturbed tree is rejected depending on which has a relatively lower probability (Huelsenbeck & Ronquist, 2003). Because Bayesian inference calculates posterior probabilities for clades, it determines support values without the need for bootstrapping (Bergmann, 2003). Bootstrapping does not facilitate comparison between equally most parsimonious cladograms, while Bayesian results are a powerful independent test for choosing between such parsimony-derived trees.

We ran the Bayesian phylogenetic analyses using MrBayes 3.0 for Macintosh OS X (Huelsenbeck & Ronquist, 2003). MrBayes incorporates the MCMC morphological model of Lewis (2001), with the modification that prior state frequency probabilities are assumed to be variable (Bergmann, 2003). The analysis ran for 1000 000 MCMC generations, with every 100 generations sampled and burnin set to 1000 (100 000 generations). 'Burnin' is the number of sampled generations the Markov chains run before the tree likelihoods reach relatively stable values ('stationarity:' Huelsenbeck & Ronquist, 2003). The chains then run for the total number of generations minus the burnin value to arrive at final posterior probability values for nodes (Bergmann, 2003). The analyses took 1.5–2 h on an 800 Mhz G3 Apple iBook. From the MrBayes output files, trees were constructed in Mesquite 0.993d42 (Maddison & Maddison, 2003) running under Macintosh OS X. NEXUS files containing the matrices and MrBayes instruction blocks are available from the first author.

RESULTS

QUALITATIVE DESCRIPTIONS

We first describe MT III of exemplars of terminal taxa and then explore notable variations within more

Table 1. Morphological variation of theropod third metatarsals. Constriction: **S**plint = parallel sided rod, with distal widening; **T**aper = converging proximally along the long axis of MT III. **Pl**antar = triangular cross section. Ligament correlates: **E**xtended (II) = distal extension of proximal MT II correlate. Proximal expansion X (cross)-section: see text. The designation n/a (not applicable) means the condition does not exist for the examined specimens

	Constriction		Ligament correlates		Prox. expansion X-sect.			
						Complex		
	Proximal: **S**plint/ **T**aper	**Pl**antar	Proximal: **F**acets **R**ugosity Extended (II)	Distal: **F**acets **R**ugosity	**Sa**gittal	**H**ooked	**P**osteriorly **w**ide	**P**ostero-**m**edial **ex**pansion
Tyrannosaruidae	**S**	**Pl**	**F, R**	**F, R** (II)		**H**	n/a	n/a
Ornithomimidae	**S**	**Pl**	**F**	**F**	**Sa.**	n/a	n/a	n/a
Troodontidae	**S**	**Pl**	**F**	**F**	**Sa.**	n/a	**P.w.**	n/a
Oviraptoridae						n/a	n/a	n/a
Rinchenia	**T** (slight)	n/a	?articulated	n/a		n/a	n/a	n/a
Ingenia	n/a	n/a	**F**		**Sa.**	n/a	n/a	n/a
Caenagnathidae		n/a				n/a	n/a	n/a
Elmisaurus	**S**	n/a	fused	**F**		n/a	**P.w.**	n/a
Chirostenotes	**T**	n/a	?articulated	?articulated		n/a	n/a	n/a
Dromaeosauridae	n/a	n/a	**F, R**	**F**	**Sa**	n/a	n/a	n/a
Carnosauria	n/a	n/a			n/a	n/a	n/a	n/a
Allosaurus	n/a	n/a	**F, R, E**	n/a	n/a	n/a	n/a	**P-m.e.**
Carcharodontosaurid	n/a	n/a	**F, R**	**F, R** (small)	n/a	n/a	n/a	**P-m.e.**
Fukuiraptor	n/a	n/a	**F**	n/a	n/a	n/a	n/a	**P-m.e.**
Sinraptor	n/a	n/a	**F, R, E**	n/a	n/a	n/a	n/a	**P-m.e.**
Basal Tetanurae	n/a	n/a		n/a	n/a	n/a	n/a	
Torvosaurus	n/a	n/a	**F, R**	n/a	n/a	n/a	n/a	**P-m.e.**

diverse clades. Description proceeds from proximal to distal along the metatarsal. Table 1 summarizes variation in the proximal articular region, attenuation of the shaft (if any), and the presence and degree of rugosity of proximal and distal ligament scars.

Theropod third metatarsals have several features in common. They usually have deep subcircular ligament fossae (for collateral ligaments between the metatarsal and the first phalanx; Ostrom, 1969) on the disto-lateral and -medial surfaces. (On the fourth metatarsal these indentations are shallow on the medial surface and often absent on the lateral surface.) Proximally on MT III, the articular surfaces for MT II and IV are rugosely striated in tyrannosaurids (Fig. 3), other large theropods (Fig. 8), and *Deinonychus*. The complementary surfaces of MT II and IV are similarly striated, probably indicating intermetatarsal ligaments in this region (Snively & Russell, 2003). We now report variations and similarities in MT III morphology, starting with tyrannosaurids.

Tyrannosauridae
Tyrannosaurus rex. MT III is hook-shaped in proximal cross section: the outline of the hook runs antero-posteriorly near the plantar surface and has a sharp lateral bend anteriorly (Fig. 3A), so that a large surface is visible in anterior view. Discrete striated ligament scars mark the articular surfaces where MT III is constrained anteriorly by MT II and posteriorly by MT IV. Distal to these articulations the metatarsal narrows to a splint. It then re-expands asymmetrically in anterior view, with a strong convex curvature medially. The metatarsal has an asymmetrically triangular cross section in this region, with its apex towards the plantar surface but offset laterally (Figs 3B, 4). The surfaces exposed in plantar view are distal articular facets with MT II and IV (Fig. 3B). The scar for MT II is wider and extremely rugose. The phalangeal articular surface is extensive proximodistally, has a primarily medially inclined proximal edge, and proximal to this edge has a deep, medially inclined reniform (kidney-shaped) indentation (Fig. 3A). Novas (1994) identified a similar indentation in *Herrerasaurus* as
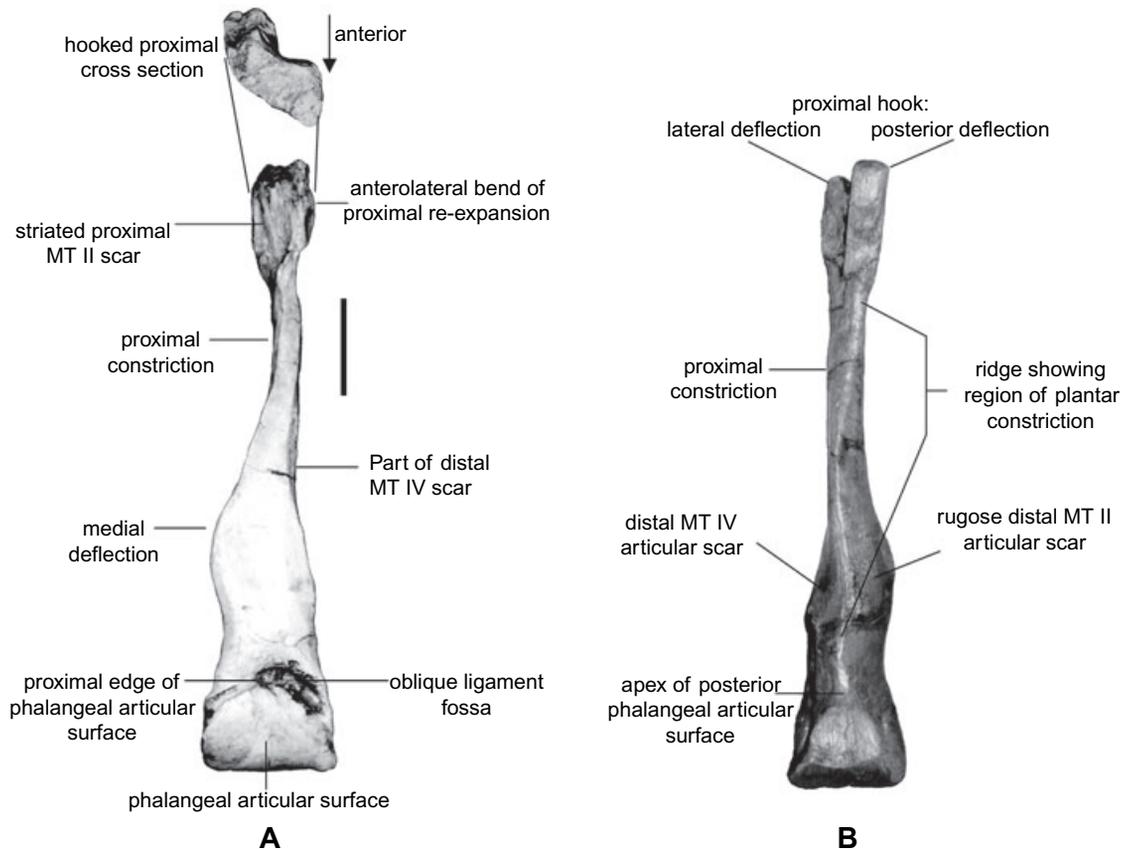
Figure 3. Morphological features of the third metatarsal (MT III) of tyrannosaurids. A, anterior view (bottom; scale bar = 10 cm) and proximal view (top), not to scale, of left *Tyrannosaurus rex* MT III. Note hooked cross section in proximal view, rugose striated scar for proximal articulation with MT II, proximal splint, and deep oblique ligament fossa. B, posterior view of left *T. rex* MT III. Distally, the metatarsal constricts to form a ridge, making the element triangular in this region. Note distal scars for ligamentous articulation with MT II and IV.
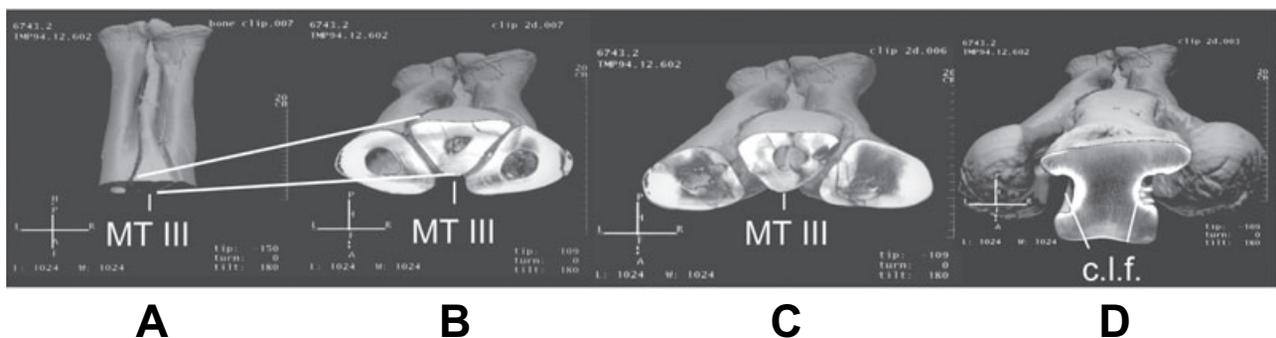

Figure 4. 3-D CT images of right *Gorgosaurus libratus* metatarsus (TMP 94.12.602), with cross sections shown at various points along the structure. A, reference image of proximal half of metatarsus. B and C, MT III becomes triangular in distal cross section. D, collateral ligament fossae (c.l.f.) for phalanx III-1.

an extensor ligament fossa. Its location and general morphology in theropods resemble the distal attachment of an anterior oblique metapodial ligament of lizards (McGregor, 2000); we hereafter refer to it as the oblique ligament fossa.

Variations. Other tyrannosaurid third metatarsals differ little from that of *T. rex*. They appear less robust and bear lighter scarring on the MT II articular facet. Some specimens of *Albertosaurus* (Fig. 9: *As.*) appear more gracile than equivalent elements of *Daspletosaurus, Gorgosaurus,* and *Tarbosaurus* of similar length.

Ornithomimidae
Proximally, MT III of ornithomimids is expanded anteroposteriorly, evident in lateral or proximal views. Faceted articular surfaces are present for MT II and IV in this region. Distally, MT III is very similar to the tyrannosaurid condition but is symmetrical mediolaterally in anterior view, has sharp edges along its lateral and medial sides, and lacks rugosity on the distal articular facets. The posterior edge of the plantar constriction is a sharp ridge (Fig. 5D), unlike the more

rounded condition in tyrannosaurids (but similar to the condition in troodontids and *Avimimus*). The oblique ligament fossa proximal to the phalangeal articular surface is very shallow, unlike in tyrannosaurids, but the proximal edge of the surface inclines medially in the same manner.

Troodontidae
Troodon formosus (Fig. 6). Proximally, MT III expands to form a triangular cross section, with the apex towards the anterior (dorsal) surface. In anterior view the proximal splint is strikingly narrow mediolaterally and long relative to the distal expansion (Fig. 6A). In contrast to the situation in tyrannosaurids and ornithomimids, the distal articular surface with MT IV is medially inclined in anterior view, and that with MT II is straight (Fig. 6B). The posterior edge of the plantar constriction is more medially deflected than it is in other arctometatarsalians but forms a sharp ridge as it does in ornithomimids (Fig. 6B). Anteriorly, the phalangeal articular surface is more symmetrical than in tyrannosaurids or ornithomimids, while this
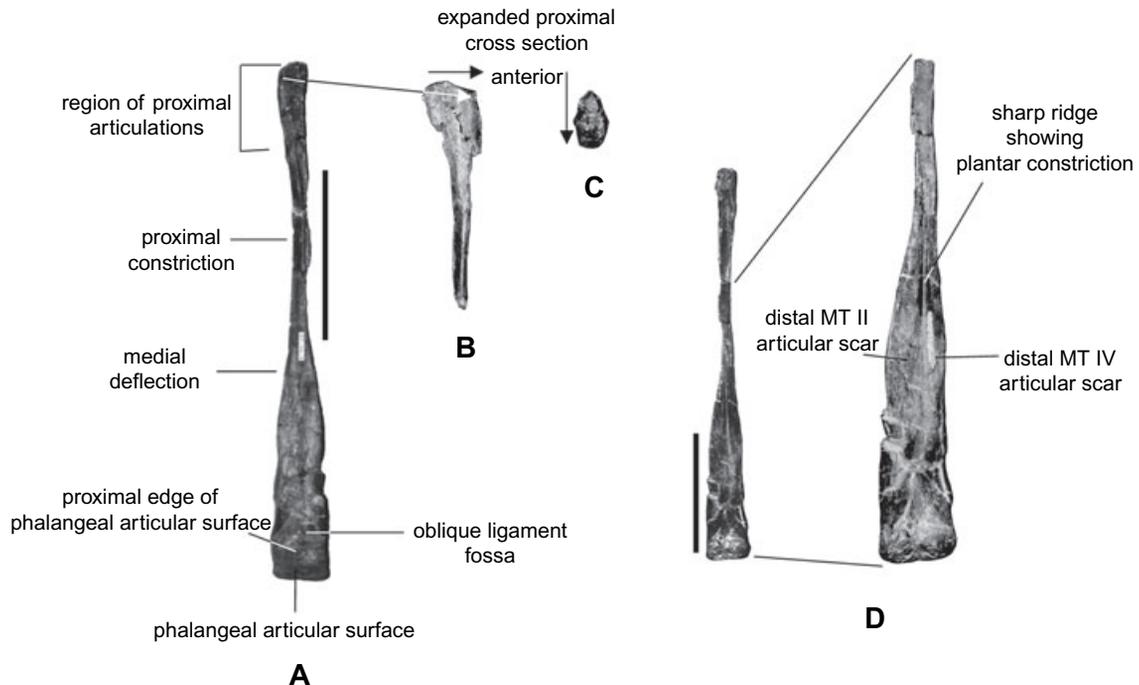

Figure 5. Morphological features of MT III of ornithomimids. Scale bars = 10 cm. A, anterior view of right ornithomimid MT III. B, proximal, anteroposterior expansion of ornithomimid MT III in medial view. Arrow shows an approximate corresponding point in the anterior view. C, proximal, anterioposterior expansion of ornithomimid MT III in proximal view. D, features of ornithomimid MT III in posterior view. Inset (left) shows the enlarged proportion of the element. Note sharp ridge of plantar constriction (right).
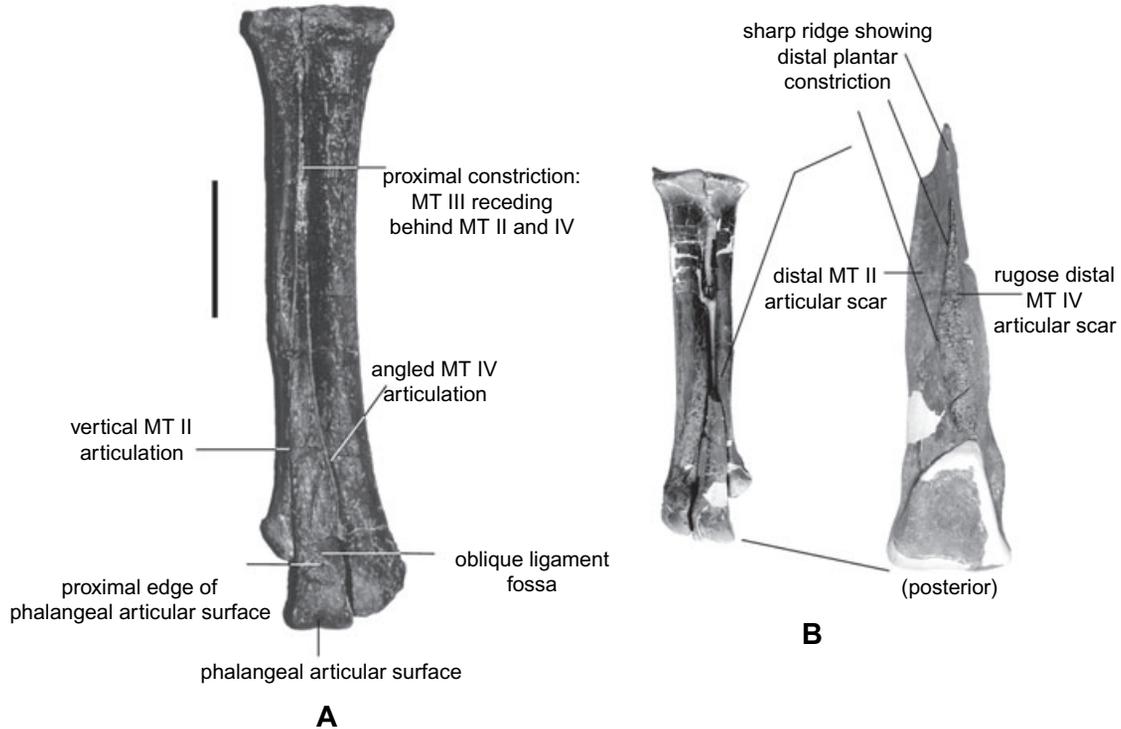
Figure 6. Morphological features of the MT III of troodontids. A, anterior view of a left metatarsus of *Troodon formosus*. MT II and MT IV obscure MT III proximally. A medially inclined distal articulation indicates high force transfer from MT III to MT IV (scale bar = 10 cm). B, posterior view of the distal portion of right *Tr. formosus* MT III. Inset (left) shows position of the enlarged portion of the element (in anterior view). Note sharp ridge of plantar constriction (right).

surface extends farther proximally in posterior view (Fig. 6).

Oviraptorosauria
Elmisaurus sp. (Fig. 7). As in troodontids, the proximal portion of MT III is narrower anteriorly (Fig. 7A) than posteriorly (Fig. 7B) but is not triangular, and this condition persists farther distally along the proximal splint. Near the mesotarsal joint MT III is fused to MT II and MT IV: the three elements grade together in posterior view (Fig. 7B). In anterior view MT III expands distally as in tyrannosaurids, ornithomimids, and troodontids but is never triangular in cross section. The phalangeal articular surface has medially and laterally expansive trochlear ridges (Fig. 7A, B).

Variations: MT III of *Chirostenotes pergracilis* (Fig. 7C) and *Rinchenia mongoliensis* (Fig. 9A: *R.m.*) are constricted proximally, but the entire element is more triangular in anterior view than is the case in *Elmisaurus* and lacks a discrete proximal splint. MT III of *Ingenia yanshini* (Fig. 9A: *I.y.*) is robust, has a slight anteroposterior expansion proximally, and is rectangular in anterior view.

Dromaeosauridae
Deinonychus antirrhropus (Figs 8, 9B: *D.a.*). MT III of *Deinonychus* is anteroposteriorly expanded near the mesotarsal articular surface and is lightly striated along the articular facets for MT II and IV. The shaft is rectangular in anterior view. There is a large distal articular facet for MT II that is slightly inclined towards the posterior (plantar) surface. The phalangeal articular surface is spool-shaped and inclined proximomedially.

Carnosauria/basal Tetanurae
Allosaurus fragilis (Fig. 9A). Proximally, MT III of *A. fragilis* is complexly expanded, wider towards the plantar surface and with an overall anterolateral inclination. In proximal view the proximal articular surface for MT II is strongly inclined anterolaterally, while that for MT IV is more sagittal. Both surfaces bear longitudinal striations. The shaft is slightly curved medially, with a poorly defined and unstriated distal extension of the MT II articular surface (Snively & Russell, 2003). The phalangeal articular surface is low in anterior view and variably symmetrical amongst specimens.
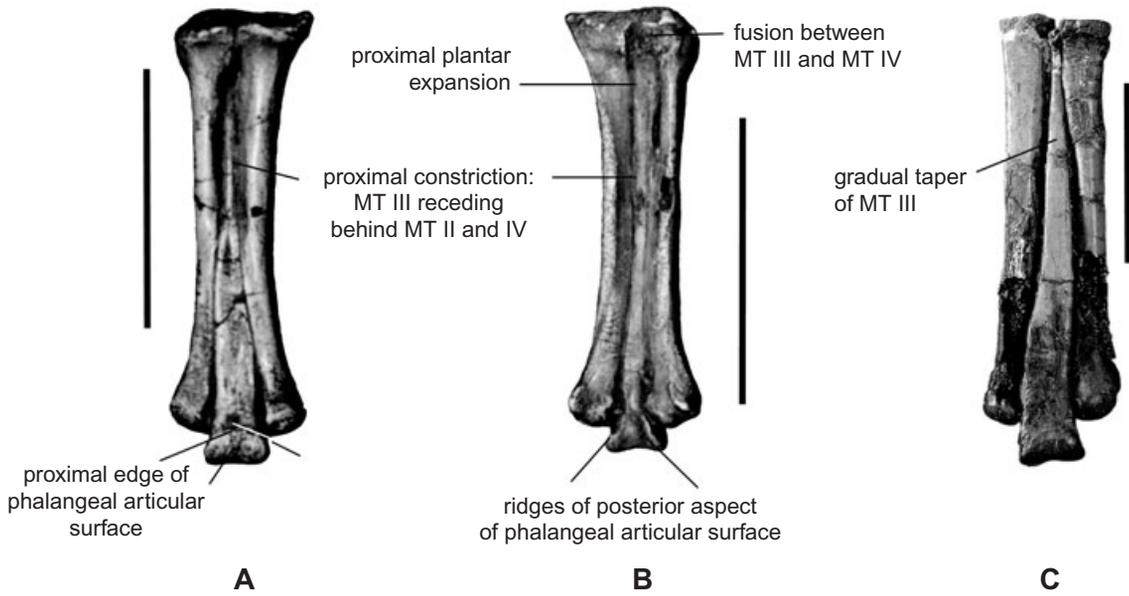
Figure 7. Morphological features of MT III of caenagnathid MT III. Scale bars = 10 cm. (A) anterior and (B) posterior views of right *Elmisaurus* sp. metatarsus. MT II–IV are fused proximally. (C) anterior view of left metatarsus of *Chirostenotes pergracilis*. MT III tapers gradually towards a proximal apex.
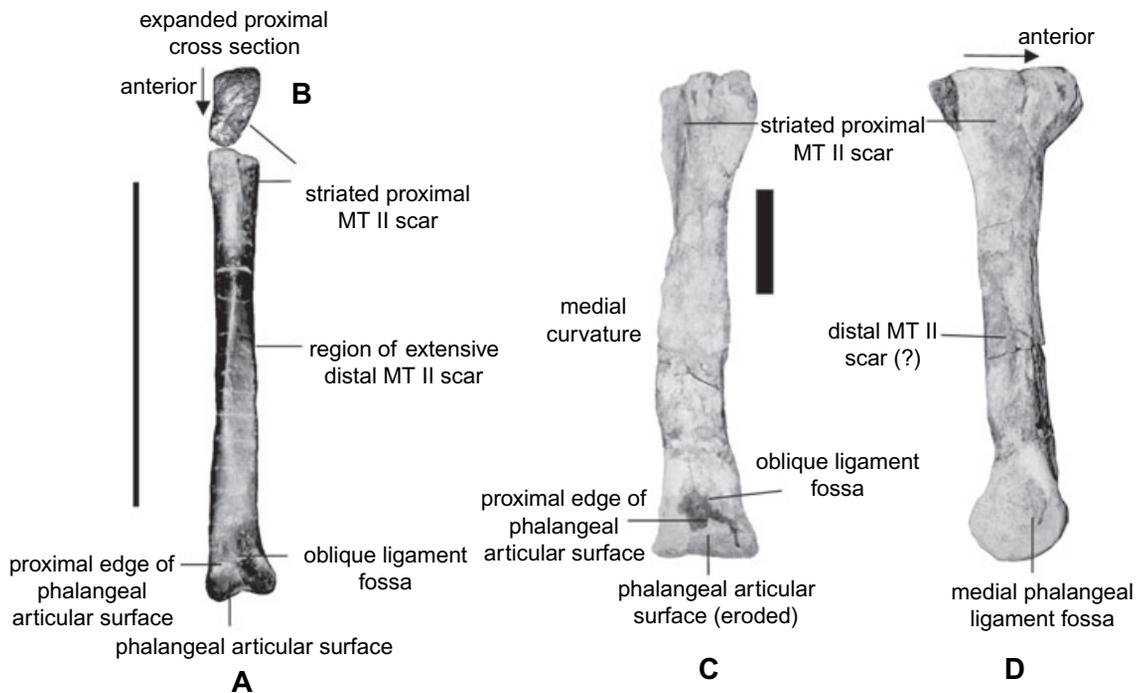

Figure 8. Morphological features of nonarctometatarsalian MT III. Scale bars = 10 cm. *Deinonychus antirrhopus* MT III in (A) anterior and (B) proximal views. Carcharodontosaurid MT III in (C) anterior and (D) medial views. For description of features see text.
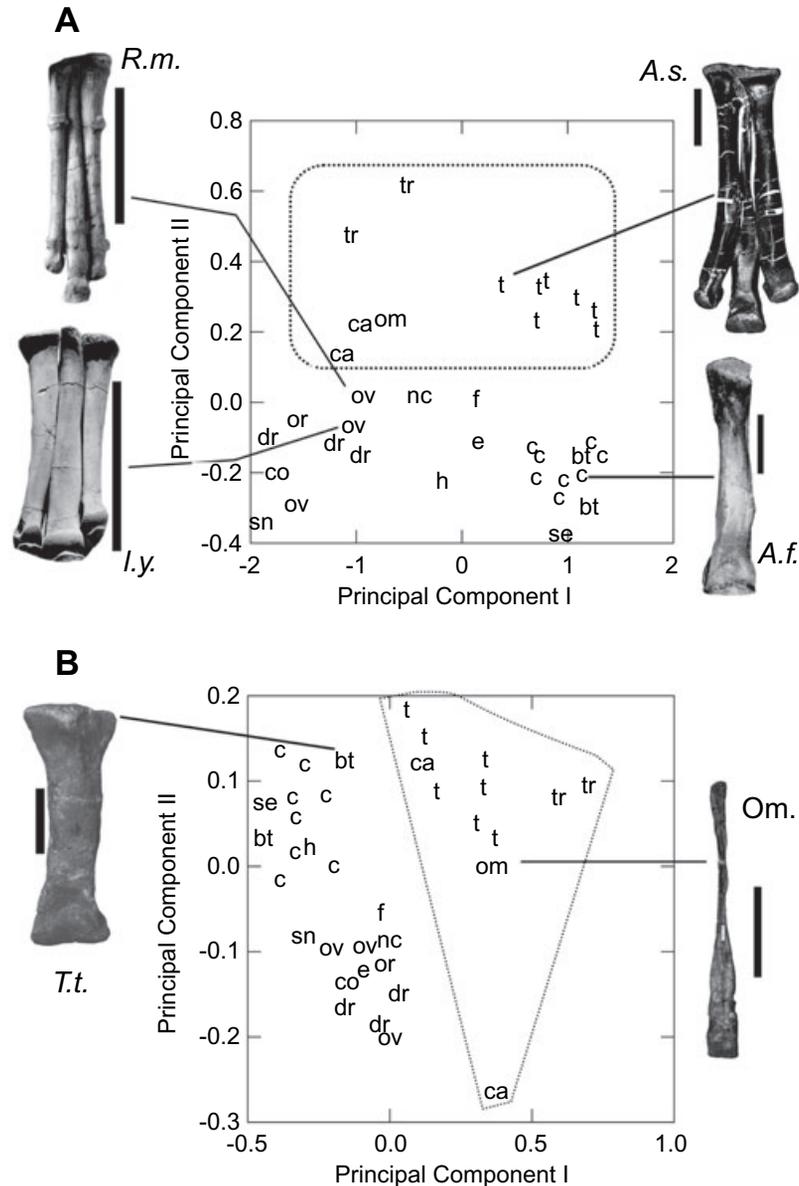
Figure 9. Results of PCA of theropod MT III. Scale bars = 10 cm. A, PCI represents size variation, and PCII indicates proximal gracility. MT III with PCII scores above 0.14 (in bevelled square) are considered arctometatarsalian. Specimens of *Albertosaurus sarcophagus* (*A.s.*), *Allosaurus fragilis* (*A.f.*), *Ingenia yanshini* (*I.y.*), and *Rinchenia mongoliensis* (*R.m.*) are figured; note differences in proximal gracility of MT III. B, results of PCA with influence of isometry removed. PCI indicates variation in proximal gracility. Arctometatarsalian forms (bevelled square) group separately from proximally robust MT III, regardless of size. MT III of an ornithomimid (*Om.*), *Deinonychus antirrhopus* (*D.a.*), and *Torvosaurus tanneri* (*T.t.*) are depicted to emphasize shape variation. *Abbreviations:* bt, basal tetanuran *Torvosaurus tanneri*; c, Carnosauria; ca, Caenagnathidae; co, *Coelophysis bauri*; dr, Dromaeosauridae; e, *Elaphrosaurus bambergi*; f, *Fukuiraptor kitadaniensis* (Carnosauria); h, *Herrerasaurus ischigualastensis*; nc, NAMAL coelurosaur; om, Ornithomimidae; or, *Ornitholestes hermani*; ov, Oviraptoridae; se, *Segnosaurus ghalbinensis*; sn, *Sinosauropteryx prima*; t, Tyrannosauridae; tr, *Troodon formosus*.

Variations: MT III of *Sinraptor dongi* is more gracile than it is in *Allosaurus* specimens, with a better defined and slightly rugose distal articular extension for MT II. A carcharodontosaurid specimen (Fig. 8) has a discrete roughened scar, presumably for distal ligamentous articulation with MT II. MT III elements of the basal tetanuran *Torvosaurus tanneri* (Fig. 9B) are very much like those of a robust *Allosaurus*.

NUMERICAL RESULTS FROM PCA

For the initial PCA, Table 2 displays the loading of each variable along the first three principal components, the percentages of the variance of each variable explained by each component, and the correlation of each variable with each component. The first three principal components account for 98.7% of total variance: PCI explains 91%, PCII 6.7%, and PCIII 1%. These three components describe significantly different aspects of the sample's total variance (Bartlett's $\chi^2 = 27.008$, 2 d.f.; $P < 0.005$), but the fourth component is isotropic with the remainder (Table 2). The three principal components derived from the original data set thus suffice to describe the size- and nonsize-associated variance exhibited by the sample.

PCI, considered as the size-dependent shape vector, describes overall MT III scaling which is significantly allometric ($\chi^2 = 117.85$, 6 d.f., $P < 0.005$). This can be principally attributed to the negative allometry of LTOTAL and the positive allometry of WPROX (Table 2). All of the variables are highly correlated with PCI and have large amounts of their total variance explained by this component (Table 2); absolute size and its associated requirements are evidently very important to the shape of the MT III over the size range of our sample. LTOTAL, W75% and HPAS have slightly lower amounts of variation explained by PCI than the remaining variables. LTOTAL has a smaller correlation with the size-associated shape component (Table 2), indicating that aspects of these variables, and of total length of MT III in particular, are affected by factors other than absolute size.

PCII explains nonsize-associated variance, and the range of correlation values and percent variance explained by this component for the variables (Table 2) do not display the uniformity of the corresponding statistics for PCI. Specimen scores do not group by the size of the original animal; carnosaurs and tyrannosaurs do not overlap along PCII, although both groups contain scores similar to those of a number of smaller taxa (Fig. 9A). Most of the remaining variance of LTOTAL is accounted for by this component (Table 2), and it has a high correlation with PCII, indicating that nonsize-associated variance in MT III length is important in distinguishing groups. Similar observations can be made concerning HPAS (Table 2), which can be expected to vary with LTOTAL. The three most proximal widths of MT III (PW, W25%, W50%) have negative loadings, and are negatively correlated with PCII. W25% is the most important of these, having the greatest amount of variance explained by PCII. Proximal MT III width thus varies inversely with MT III length, and nonsize-associated variation in W25% contributes to differences among taxa. Overall, from its relationship with proximal width and total length variables, this component can be said to describe MT III proximo-distal gracility.

PCII is best examined with the influence of isometry removed (Table 3; PCI and PCII here correspond to PCII and PCIII in the previous analysis, although in the isometry-removed PCA there is no component corresponding to PCI in the original PCA). Of the total sample variance remaining when the effect of isometry is removed (8.54% of the original total variance), over 68% is explained by PCI, which also generally explains much of the remaining variance for each variable and displays high correlations with each (Table 3). The loadings of PCI indicate that the proximal widths of MT III, to the midpoint of the bone,

Table 2. First three components of PCA of theropod MT III measurements (determined to be informative; PCIII–VII Bartlett's $\chi^2 = 199.87$, 14 d.f.; $P < 0.001$; PCIV–VII Bartlett's $\chi^2 = -164.82$, 9 d.f.; NS), with loading values for each variable, percentage of total variance of each variable explained by each component, and correlation of each variable with each component. Variable names as defined in the text

	Loadings			Variation per component			Component correlations		
	I	II	III	I	II	III	I	II	III
LTOTAL	0.272	0.454	−0.112	0.83	0.169	0.002	0.911	0.411	−0.04
PW	0.43	−0.313	−0.804	0.928	0.036	0.036	0.976	−0.192	−0.193
W25%	0.388	−0.522	0.237	0.88	0.117	0.004	0.98	−0.357	0.063
W50%	0.374	−0.347	0.438	0.928	0.058	0.014	0.97	−0.243	0.12
W75%	0.393	0.229	0.303	0.969	0.024	0.006	0.958	0.151	0.078
DW	0.411	0.228	−0.012	0.978	0.022	0	0.997	0.15	−0.003
HPAS	0.358	0.445	0.017	0.898	0.102	0	0.949	0.319	0.005
Eigenvalues	0.885	0.065	0.01						
% variance explained	91.036	6.653	1.017						

Table 3. First two components of PCA of theropod MT III measurements (determined to be informative; PCII–VII Bartlett's χ^2 = 156.96, 20 d.f.; $P < 0.001$; PCIII–VII Bartlett's χ^2 = –140.75, 14 d.f.; NS by Bartlett's χ^2). These components are derived from data from which variance due to geometric similarity has been removed, with loading values for each variable, percentage of total variance of each variable explained by each component, and correlation of each variable with each component. Variable names as defined in the text

	Loadings		Variance per component		Component correlations	
	I	II	I	II	I	II
LTOTAL	0.504	−0.49	0.756	0.138	0.862	−0.369
PW	−0.373	0.537	0.575	0.231	−0.755	0.479
W25%	−0.52	−0.339	0.923	0.076	−0.927	−0.266
W50%	−0.343	−0.386	0.755	0.184	−0.805	−0.398
W75%	0.172	0.137	0.499	0.061	0.612	0.214
DW	0.152	0.415	0.351	0.506	0.526	0.632
HPAS	0.408	0.126	0.976	0.018	0.877	0.119
Eigenvalues	0.069	0.013				
% variance explained	68.45	13.234				

decrease with increasing LTOTAL, while the more distal widths and HPAS increase (Table 3). MT III thus displays marked variation in proximal gracility that is independent of overall size.

PCIII in the isometry-removed PCA explains less than 10% of the total remaining variance and defines no more of an axis than PCIV of the isometry-removed PCA (Bartlett's χ^2 = 1.871, 2 d.f.; $P > 0.05$). The variance that PCIII explains for WPROX, and to a lesser extent W50% and W25%, cannot be attributed with any certainty to such factors as phylogeny or adaptation. However, the relatively large amount of the remaining variance explained by this component for these three variables, and the negative correlations with WPROX and WDIST (Table 3), indicate that PCIII describes the degree to which specimens resemble a top- or bottom-heavy hourglass. This suggests that aspects of distal robustness in MT III not related to the proximal gracility described by PCII are of some importance.

Plotting specimens' PCI scores from the second PCA against isometry-removed values for their measured variables reinforces the allometric importance of LTOTAL and W25%. Most carnosaurs and basal tetanurans have very small LTOTALs after the removal of isometric size, whereas the similarly sized tyrannosaurids retain greater amounts. Troodontids retain the greatest amount of LTOTAL after the removal of isometric variance. In contrast, carnosaurs and basal tetanurans display the greatest W25% after isometric size is removed and troodontids the least. These results confirm, independently of clustering, the overall and proximal gracility of the arctometatarsalian MT III regardless of its absolute size.

GROUPING OF SPECIMENS BY PCA

Figure 9A plots specimen PC scores along PC axes derived from the unmodified data set, illustrating that PCI in this analysis accounts for variance associated with overall size. Tyrannosaurids, *Torvosaurus*, and larger carnosaurs, all of which have metatarsals of large absolute size, have the highest PCI scores, while the smallest specimens (*Coelophysis*, *Ingenia, Ornitholestes, Sinosauropteryx*, and *Bambiraptor*) have the lowest. All other specimens plot along PCI according to their absolute size and general robustness. Figure 9A also shows evident demarcations between subgroupings of metatarsal morphology with clustering along PCII (an index of proximal gracility). We now outline these groups in detail; taxonomic acronyms refer to those in Figure 9.

1. 'Arctometatarsalian' third metatarsals (Figs 3–7, 9A). By addressing overall size and robustness PCA might independently falsify this character state's validity, and therefore the clustering result is more than a circular corroboration of visually evident variation. Tyrannosaurids (Figs 3, 4, 9: *A.s.*, t), the ornithomimid (Figs 5, 9: om, 10A), *Troodon* (Figs 5, 9: tr), *Elmisaurus*, and *Chirostenotes* (Fig. 9: c), the third metatarsals of which have relatively narrow proximal measurements (Appendix 2), all have component scores for PCII above 0.14. The proximal narrowing clusters them despite great variation in absolute measurements and PCI scores, indicating that differences in robustness and size do not overwhelm the qualitatively identified arctometatarsalian condition. Surprisingly, all but the largest tyrannosaurid MT III (FMNH PV 2081)

have higher PCII scores than the ornithomimid, and the gradually tapering MT III of *Chirostenotes* has a higher PCII score (0.226) than that of *Elmisaurus* (0.143). The specimens of *Troodon*, with proximally the most gracile metatarsals, have the highest component scores for PCII.

2. Oviraptorosauria (Fig. 9: ov) (Oviraptoridae (*Ingenia*, cf. *Oviraptor*) + Caenagnathidae (*Chirostenotes, Elmisaurus*)), Therizinosauridae (*Segnosaurus*: se), Dromaeosauridae (dr) (*Bambiraptor, Deinonychus*), *Ornitholestes* (ol), and *Sinosauropteryx* (sn). These coelurosaurs show great diversity in MT III shape. *Chirostenotes* and *Elmisaurus* (Fig. 7), which are qualitatively considered arctometatarsalian (Holtz, 1994, 1995), show the highest values for PCII among oviraptorosaurs. The oviraptorid *Ingenia* (Fig. 9A: *I.y.*) shows high variability (PCII values of −0.22 and −0.06), while *Rinchenia* (Fig. 9A: *R.m.*) is intermediate between *Ingenia* and *Elmisaurus* (Fig. 7). *Ornitholestes* and the dromaeosaurids *Deinonychus* (Figs 8, 9B: *D.a*) and *Bambiraptor* are undifferentiable from the oviraptorosaur cluster. In contrast, MT III of the therizinosaurid *Segnosaurus* (se) is set apart from its oviraptorosaur sister group in both size (PCI) and shape (PCII), lying close to the cluster of the carnosaurs (c) and *Torvosaurus* (Fig. 9: bt). Its PCI component score value is fairly high at 0.73, and its PCII value is the lowest of any of the examined theropods, at −0.37. Unexpectedly, the small *Sinosauropteryx* has the second highest proximal robustness of MT III, with a PCII value of −0.33.

3. Carnosauria (c, f for *Fukuiraptor*; Fig. 9) and *Torvosaurus* (Fig. 9B: *T.t.*, bt). These are all relatively large theropods, and cluster strongly along PCI. Their third metatarsals show more variation in shape than those of the similarly sized tyrannosaurids, however, and are spread out farther along PCII. Surprisingly, the large carcharodontosaurid specimen (Fig. 8) is the most proximally gracile and has the highest PCII score of the group (−0.11), aside from that of *Fukuiraptor*.

4. Basal Tetanurae (Fig. 9A: bt). These are distributed within the main cluster of large carnosaurs.

5. Outgroups to Tetanurae (Fig. 9). *Herrerasaurus* (h), *Coelophysis* (co) and *Elaphrosaurus* (e) group closely along PCII, but the lower PCII scores of *Herrerasaurus* and *Coelophysis* indicate that their MT IIIs are more robust proximally.

GROUPING WHEN SIZE EFFECTS ARE MINIMIZED

A plot of the principal component scores derived from the isometry-removed data set (Fig. 9B) illustrates groupings of metatarsal morphology emphasizing the effects of taxon-specific allometry and proximo-distal shape variation rather than overall size. PCI can be interpreted as an index of proximal gracility. PCII in this analysis (describing little of the total variance, of uncertain attribution, but mainly involved with distal robustness – Table 3) does not give component scores producing obvious patterns against PCII (Fig. 9). Forms with an arctometatarsus cluster along PCI but spread widely along PCII. This result strongly indicates that arctometatarsalian third metatarsals display a consistent proximal gracility regardless of size and also indicates some small variance in allometric distal robustness of MT III among these taxa.

The clustering patterns in Figure 9B suggest that the shape of MT III in the troodontids, ornithomimids, tyrannosaurids, and caenagnathids is affected by taxon-specific allometry to a much greater degree than in the other theropod taxa, although some of the more gracile forms approach the arctometatarsalian distribution. However, robust arctometatarsalians do not overlap robust nonarctometatarsalians in this regard, nor do most gracile arctometatarsalians overlap with gracile nonarctometatarsalians (Fig. 9B). Among the nonarctometatarsalians, the robust forms are strongly separated from the gracile forms by proximo-distal shape variation (PCI), although this is not true of gracile and robust arctometatarsalians for the most part (Fig. 9B).

THIN-PLATE SPLINE COMPARISON OF *TROODON*, *TYRANNOSAURUS* AND ORNITHOMIMID THIRD METATARSALS

TPS results (Fig. 10) depict nonaffine (distortional) transformations of coordinates for *Troodon formosus*, *Tyrannosaurus rex* and the ornithomimid MT III in the region of their plantar constriction. (TPS calculates intermediate reference forms to aid assessment of transformations, but these were not useful for investigating mechanical variation between the three physical specimens.) The ridge of the plantar constriction shifts from inclining proximomedially in *Tr. formosus* to proximolaterally in the other taxa (Fig. 10C, D). This indicates a larger distal MT III–MT IV contact in the troodontid than for MT III–MT II and a larger MT III–MTII articulation in the ornithomimid and tyrannosaurid. Higher TPS bending energies indicate a more marked shift from the troodontid to tyrannosaurid morphologies (Fig. 10B, C) than between the troodontid and ornithomimid (Fig. 10D). Similarly, high energies for transforming coordinates of the lateral and medial edges of MT III between *T. rex* and *Tr. formosus* (Fig. 10B) or the ornithomimid (not shown) indicate proportionally much larger distal intermetatarsal articulations in the tyrannosaurid.
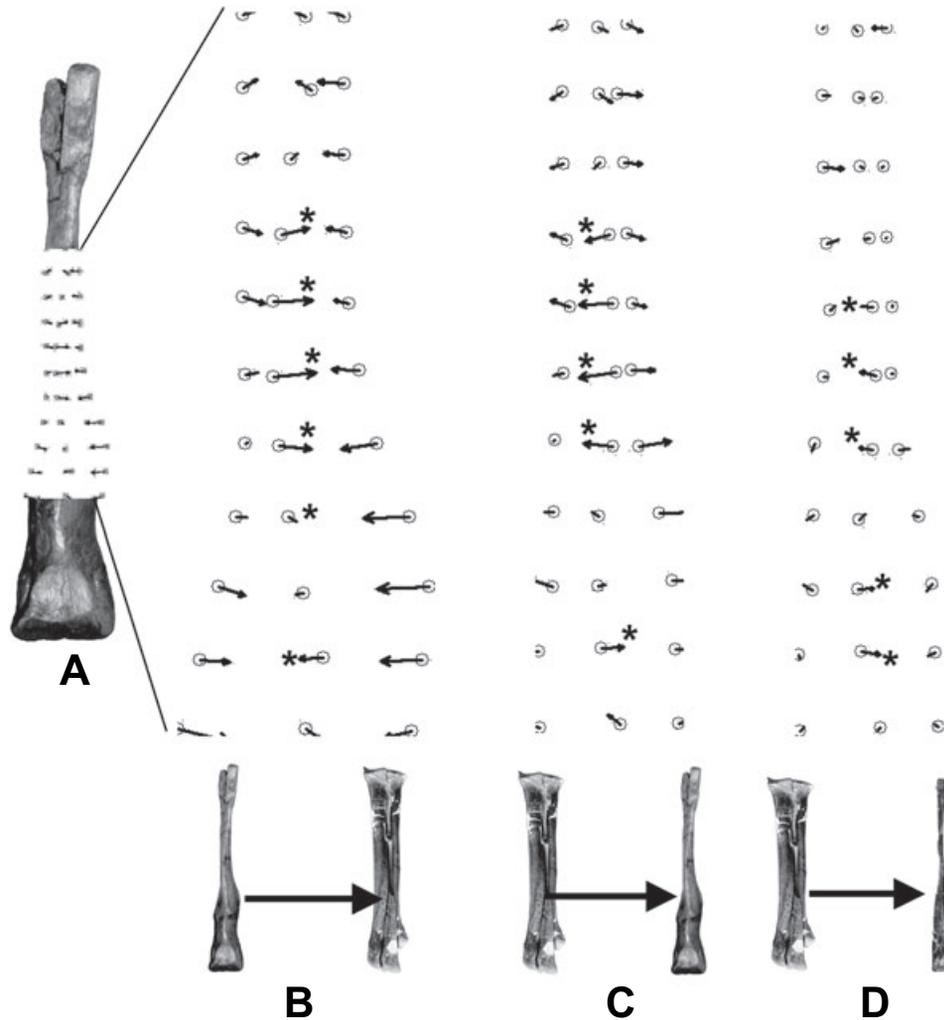
Figure 10. Results of thin-plate spline analysis. Icons (below) depict MT III specimens involved in each transformation. A, partial warp transformation of *Tyrannosaurus rex* to *Troodon formosus* MT III coordinates, overlying *T. rex* MT III from Fig. 1C. B, same transformation in A. Large arrows show high energy necessary to shift plantar constriction coordinates, mainly from lateral (*T. rex*) to medial (*Tr. formosus*). C, partial warp transformation of *Tr. formosus* to *T. rex* MT III coordinates. Large arrows show shift of plantar constriction coordinates mainly from medial (*Tr. formosus*) to lateral (*T. rex*). D, partial warp transformation of *Tr. formosus* to ornithomimid MT III coordinates. Identified arrows show shift of plantar constriction coordinates in the same directions as in C.

BAYESIAN RESOLUTION OF CONFLICTING TREES FOR THEROPODA

Figure 11 depicts the phylogenetic results of the Bayesian inference analysis of Holtz's (2000) matrix, for theropod clades whose MT III is described in this study. Because the carcharodontosaurid MT III was not identified to genus level, *Giganotosaurus + Carcharodontosaurus* is here represented as the Carcharodontosauridae. Posterior probability support is 100% for many nodes. The results differ from the strict consensus parsimony tree of Holtz (2000) and support

half of his most parsimonious trees, in that Troodontidae is united with Ornithomimosauria (Bullatosauria: Holtz, 1994, 2000) with 0.82 probability. Bayesian results also strongly support a Tyrannosauridae + Bullatosauria clade (0.83 probability). Conversely, support is poor for several trees in a later analysis (Holtz, 2001), in which Compsognathidae is the sister clade of Tyrannosauridae + Bullatosauria.

Optimization of the arctometatarsus, with full plantar and proximal constriction, shows two instances of independent evolution by this phylogeny ('Arcto.' Fig. 11), within Artometatarsalia and
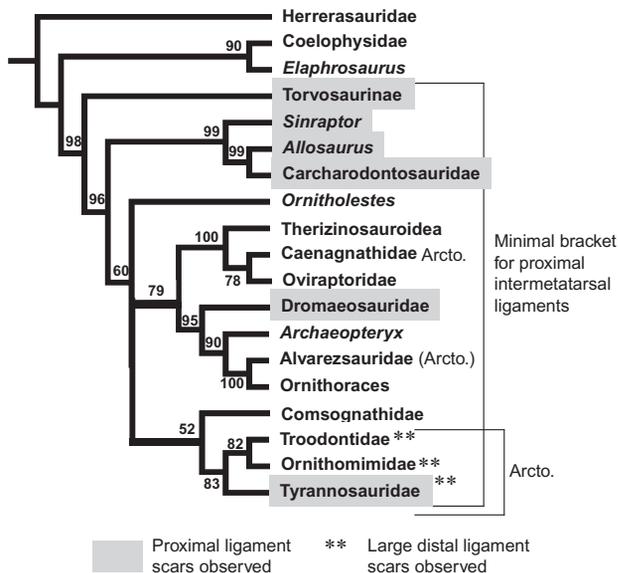
Figure 11. Bayesian inference-derived phylogeny after matrix of Holtz (2000), showing distribution of the arctometatarsus and observed ligament correlates on theropod metatarsals. Posterior probabilities (in percent) are shown at each node. 'Arcto.' designates a complete arctometatarsus, while '(Arcto.)' indicates a variant of the morphology. Taxa with proximal intermetatarsal striations are highlighted in grey, and double asterisks signify distal ligament correlates. Phylogenetic bracketing (Witmer, 1995) indicates the presence of proximal intermetatarsal ligaments in taxa between *Torvosaurus* and Tyrannosauridae. This condition is interpreted as preceding the evolution of distal ligaments in the arctometatarsus. Outgroup comparison indicates broader distribution of proximal metatarsus ligaments in the Dinosauria (see text).

Caenagnathidae. A similar structure, with MT III restricted distally, evolved in alvarezsaurids ['(Arcto.)', Fig. 11].

The Bayesian analysis of Clark *et al.*'s (2002) matrix strongly corroborates their parsimony results in separating Troodontidae from Ornithomimosauria. However, with 0.85 probability, Troodontidae falls out as part of a trichotomy with sister taxa Avialae and [Alvarezsauridae + (Oviraptorosauria–Therizinosauria–*Incisivosaurus*)]. *Sinornithosaurus* is the sister taxon to this large trichotomy, rendering Dromaeosauridae paraphyletic. Dromaeosauridae is no better resolved in the Bayesian analysis than in Clark *et al.* (2002), but interrelationships within most other clades are similar, with high posterior probability support (Fig. 12).

This phylogeny indicates more extensive homoplasy of the arctometatarsus ('Arcto.', Fig. 12), with the structure evolving in tyrannosaurids, ornithomimids, and troodontids independently. *Garudimimus* displays plantar but not proximal constriction of MT III

(photographs courtesy Y. Kobiyashi), showing that this aspect of MT morphology may have evolved before plantar constriction in Ornithomimosauria. Arctometatarsus-like morphologies ['(Arcto.)', Fig. 12] evolved independently in caenagnathids, alvarezsaurids and *Sinornithosaurus millenii* (Xu, Wang & Xu, 1999).

DISCUSSION

The descriptive and morphometric techniques are variably applicable for characterizing variation between theropod third metatarsals. PCA reveals a threshold of proximal constriction that denotes an arctometatarsalian MT III (a PCII value above 0.14 in the first analysis; Fig. 9) and quantifies the range of constriction between tyrannosaurids and ornithomimids vs. troodontids. The PCA results alone are insufficient, however, for eliciting or testing many hypotheses of functional variation.

For example, descriptive and TPS results suggest differing modes and magnitudes of energy transfer between MT III and MT II and IV in ornithomimids, troodontids and tyrannosaurids. Size and rugosity of distal intermetatarsal facets were likely proportional to articulation strength (Snively & Russell, 2003), and indicate hypotheses of mechanical scaling. Energies of footfall transduced to intermetatarsal ligaments (Snively & Russell, 2002) varied with body mass, locomotor velocity, and/or differential loading on respective digits. We address these possibilities below with reference to TPS and observed variation, but the hypotheses will require more extensive biomechanical testing. As more specimens accrue, the evolution and ontogeny of mechanical scaling will become further testable through biomechanics and phylogenetic methods.

The Bayesian inference results from this study (Figs 11, 12) corroborate extensive homoplasy of the arctometatarsus, documented by parsimony results at high taxonomic resolution (Clark *et al.*, 2002), and with vitally thorough consideration of outgroup choice (Holtz, 2001). The following discussion integrates phylogenetic and morphological results to explicate hypotheses of arctometatarsus evolution.

ARE HYPOTHESES OF ARCTOMETATARSALIAN FORM AND PHYLOGENY CORROBORATED?

Ha: Metatarsi classified as arctometatarsalian have a significantly greater degree of proximal MT III constriction than do those of other theropods

Evaluation of this hypothesis relies on both statistical and descriptive data. The small number of specimens
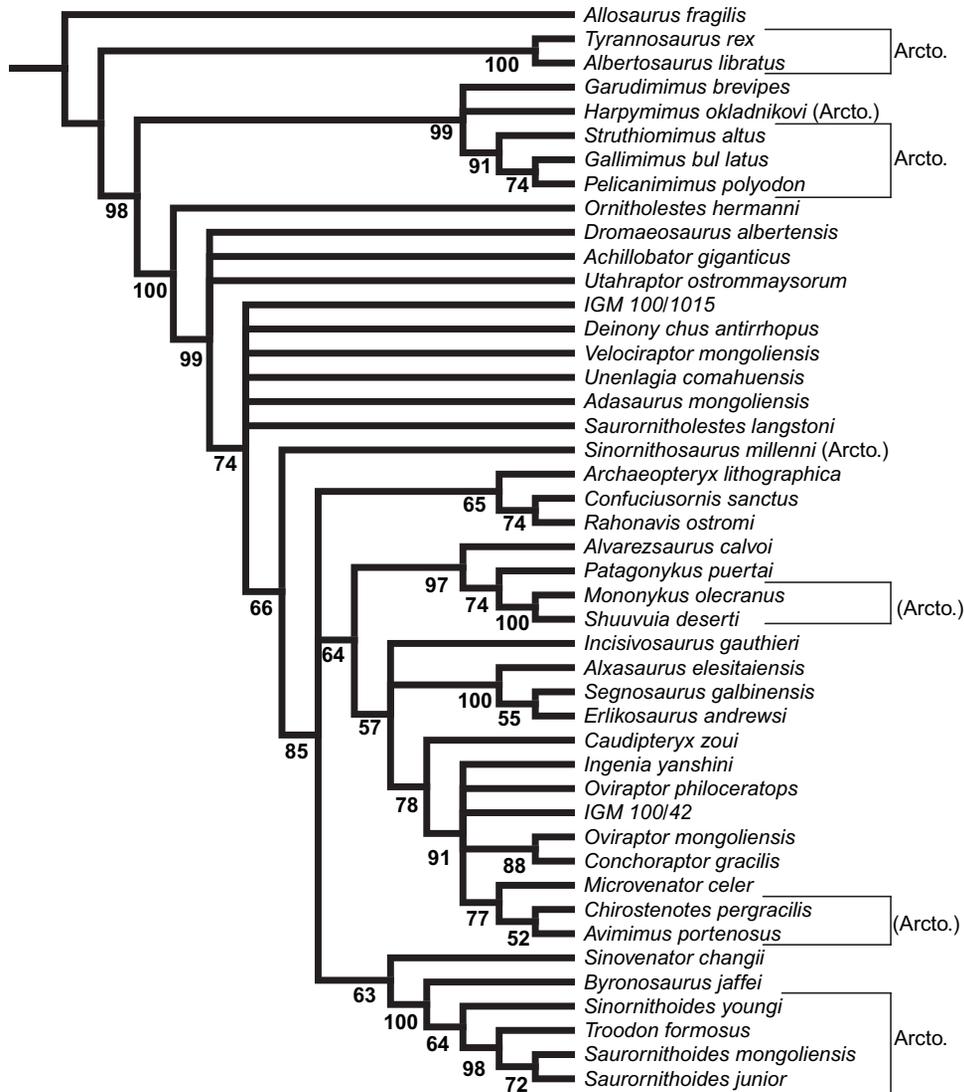
Figure 12. Genus-level Bayesian inference phylogeny from matrix of Clark *et al.* (2002), showing arctometatarsus distribution within the Coelurosauria. Percentage posterior probabilities are shown at nodes. 'Arcto.' designates a complete arctometatarsus, while '(Arcto.)' indicates a variant of the morphology.

in specific clusters of the PCA does not allow reliable use of statistical measures of aggregation. Nevertheless, the data show a striking pattern of separation along PCII (Fig. 9). We predict that a larger sample will not significantly alter the pattern of clustering.

As noted above, PCII in this analysis can be soundly interpreted as an index of proximal gracility. Tyrannosaurids, the ornithomimid, and *Troodon formosus* all have PCII values above 0.22 (Fig. 9), substantially higher than those of theropods identified as nonarctometatarsalian (Holtz, 1994, 1995; Fig. 9). The hypothesis is therefore strongly corroborated for these taxa.

However, the PCII value for the caenagnathids *Elmisaurus* and *Chirostenotes* (Figs 7, 9) is intermediate between that of the ornithomimid (Fig. 9: om) and *Rinchenia* (Fig. 9A: *R.m*). If PCII values were the only criteria for shape clustering, the *Elmisaurus* MT III would be revealed as gradationally transitional between other proximally pinched forms and *Rinchenia*. The hypothesis would therefore be falsified for caenagnathids. However, observation and close examination of the PCA results indicate that MT III of these forms are proximally constricted and distally buttressed by MT II and IV. Measurement and observation of the *Elmisaurus* MT III show that the element becomes more robust proximally in posterior view, which accounts for its intermediate PCII score despite a classically arctometatarsalian appearance.

Hb: Arctometatarsalian MT III are phylogenetically differentiable in their degree of relative proximal constriction, in accordance with the hypotheses of relationship in Figure 1

PCA falsifies this hypothesis for tyrannosaurids and ornithomimids, and somewhat less compellingly for troodontids. The similarity of size-inclusive PCII scores (and PCI scores in the isometry-removed analysis) indicates that MT III of tyrannosaurids and ornithomimids are not differentiable based on proximal constriction alone. This congruence was not necessarily predictable from visual inspection of the metatarsals, although they all share the arctometatarsalian mien in gross proportions. Sereno (1999) and Clark *et al.* (2002) find support for separate arctometatarsal origins in ornithomimids and tyrannosaurids, a compelling hypothesis in part because sister groups to Ornithomimidae (*Harpymimus* and *Garudimimus*) lack all defining traits of the morphology. Employing these phylogenies, PCA results indicate remarkable convergence of proximal MT III constriction in these taxa ('Arcto.' in Fig. 1A).

Conversely, Holtz (2000, 2001) and the corresponding Bayesian analysis in this study corroborate a single origin of arctometatarsalian MT III proximal constriction, plantar constriction, and exclusion from the proximal surface of the metatarsaus in a clade including tyrannosaurids and ornithomimids (Arctometatarsalia; Holtz, 2001; 'Arcto.' in Fig. 1B). Holtz's (2000, 2001) character evidence indicates reversal of these traits in *Harpymimus* and *Garudimimus* (Holtz, 2001). Our Bayesian results support this hypothesis. However, Holtz (2000) subsumed *Harpymimus* and *Garudimimus* within an Ornithomimosauria polymorphic for the arctometatarsus. If *Harpymimus* and *Garudimimus* are coded separately, Bayesian analysis may indicate that an arctometatarsus evolved in derived ornithomimosaurs but was not present basally within the clade.

Our Bayesian results from Holtz's matrix and half of Holtz's (2000) equally parsimonious trees situate Troodontidae within Arctometatarsalia. However, the remainder of his parsimony trees, the results of Sereno (1999), and parsimony and Bayesian results for the Clark *et al.* (2002) matrix contradict this hypothesis. The Clark *et al.* (2002) matrix provides strong falsifying evidence, since it incorporates the basal troodontid *Byronosaurus* that lacks the bulbous parasphenoid of ornithomimosaurs and more derived troodontids. Troodontids are aligned with birds in our Baysian results from the Clark *et al.* (2002) matrix, but irresolution within the Dromaeosauridae signals caution in accepting this result. MT III of *Troodon* have higher PC scores for proximal gracility than do ornithomimids and tyrannosaurids, but score much closer to gracile tyrannosaurids than to most other

coelurosaurs. *Troodon*'s arctometatarsalian PC scores are striking given a homoplasious origin under most hypotheses and the great difference in size-included PCII scores for *Troodon* and other deinonychosaurs (*sensu* Gauthier, 1986; Sereno, 1999; Clark *et al.*, 2002).

Unlike in ornithomimids and tyrannosaurids, the hypothesis that MT III constriction differs in accordance with phylogeny is clearly valid for caenagnathids. The lower size-inclusive PCII scores for *Chirostenotes* and *Elmisaurus* contradict the proximal constriction as a reliable synapomorphy linking them to the three previous taxa. The phylogeny of Clark *et al.* (2002) does not include *Elmisaurus*. Nevertheless, their placement of *Chirostenotes* within the Oviraptorosauria concords with its (unusual) proximally narrow MT III originating separately from that of other coelurosaurian clades. Holtz (2000, 2001) also places caenagnathids within the Oviraptorosauria, indicating a separate origin for proximal narrowing of MT III in Caenagnathidae vs. other taxa. Proximal fusion of the metatarsus and proximal tarsals of *Elmisaurus* and the gradual taper of MT III in *Chirostenotes* make it difficult to evaluate the element's condition in their common ancestor. Their differing morphologies may indicate independent origins of MT III constriction within the Caenagnathidae. More skeletal material is needed to test this hypothesis.

Other qualitative character states are more useful as potential troodontid, ornithomimid, and/or tyrannosaurid synapomorphies and autapomorphies. Troodontid and ornithomimid MT III share a sharp edge to their plantar constrictions (Figs 5, 6). Tyrannosaurid MT III have a deep and medially inclined oblique ligament fossa just proximal to the phalangeal articular surface (Fig. 3). This characteristic does not occur in other theropod MT III regardless of size or regional robustness. We therefore interpret this feature as autapomorphic for tyrannosaurids and not the product of a biomechanically induced allometric signal common to all considered taxa.

The proximal re-expansion of MT III also differs greatly between tyrannosaurids and other relatively gracile forms. In the tyrannosaurid MT III, the region of proximal articulation with MT II and MT IV is hooked in cross section (Paul, 1988; Holtz, 1995). An *Albertosaurus sarcophagus* MT III that is unusually narrow near the ankle displays this morphology, while similarly gracile ornithomimid specimens do not. This evidence suggests that a proximally hooked MT III is not simply an artefact of positive allometry in arctometatarsalians and is useful as a discrete character state diagnosing tyrannosaurids (Holtz, 2000).

It is possible that some form of complexly expanded proximal MT III is symplesiomophic for Coelurosauria, since variants occur in the basal tetanuran

Torvosaurus tanneri, carnosaurs, and the coelurosaurian tyrannosaurids and *Ornitholestes*. Paul (1988, 2002) notes that a hooked MT III may diagnose a tyrannosaurid-*Allosaurus*-*Ornitholestes* clade. However, unhooked (though posteriorly expanded) proximal MT IIIs occur in carnosaurs other than *Allosaurus*, and most independent character evidence (Holtz, 1994, 2000, 2001; Sereno, 1999) suggests that a complexly expanded proximal MT III is homoplastic in carnosaurs and tyrannosaurids.

IS MT III SHAPE SEGREGATION FUNCTIONALLY INFORMATIVE?

There is a strong tradition of inferring function from structure in fossil organisms. Morphological clustering can imply but not demonstrate similarity of function, an inference fraught with complications even in studies of modern organisms (Lauder, 1995). Particularities of skeletal and soft tissue anatomy and unforeseeable pleiotropic roles for an organ will reduce the reliability of functional inference in fossils. This caveat applies to fossil structures with likely analogous function in modern homologues, but it will especially impede inferences about organs that are structurally diverse in extant and extinct members of a clade.

However, possible biomechanical actions of structures are readily deducible from their morphology. Morphometrics can test hypotheses of metatarsus function, such as the following.

(Hc): Tyrannosaurids, troodontids, and ornithomimids differed in modes of footfall energy transmission

Thin-plate spline (TPS) analysis indicates that the ridges of MT III plantar constriction in ornithomimids, troodontids, and tyrannosaurids are variably offset from the element's sagittal midline (Fig. 10). The lateral offset in the tyrannosaurids and ornithomimid signifies a larger articulation between MT III and MT II than between MT III and MT IV, which corresponds with larger measured areas of articular surfaces at the MT III–MT II joint (Snively & Russell, 2003) and larger inferred cross sectional area of MT III–MT II ligaments.

Assuming that stress (force/area) on intermetatarsal ligaments was similar across both articulations, larger MT III–MTII areas indicate that greater footfall force was transmitted through this joint than that between MT III and MT IV, and that MT II experienced greater locomotor forces than MT IV. Greater phalangeal articulation surface area on MT II than MT IV corroborates this hypothesis for tyrannosaurids (Snively & Russell, 2002). The smaller lateral offset of the constriction ridge of the ornithomimid

MTIII, and less medial displacement of the medial edge of the metatarsal, indicate that the respective facets for MT II and IV were closer in size than in tyrannosaurids. Correspondingly similar intermetatarsal ligament areas indicate that forces transmitted to MT II and IV were more evenly matched in ornithomimids than in the other taxa.

In troodontids the plantar ridge is more medially offset than in ornithomimids or tyrannosaurids, resulting in a proportionally larger MT III–IV articulation and greater ligament area that between MTIII and MTII. Comparatively larger footfall energies were undoubtedly channelled from MT III to MT IV in troodontids. This is logical, since their hyperextensible digit II was probably not load-bearing.

Tyrannosaurids display a greatest degree of rugosity on their distal intermetatarsal facets, indicating particularly strong and resilient ligaments (Snively & Russell, 2003) consistent with the large size of these animals. The troodontid MT III has an expectedly rugose distal facet for MT IV, while intermetatarsal articular surfaces are smooth in examinable ornithomimid specimens (TMP 87.54.1; TMP 2002.45.64; TMP field station, uncatalogued). We predict that intermetatarsal ligament scars will be rugose in large ornithomimids for stronger articulation as these animals scaled higher in body mass.

OTHER ASPECTS OF MT III FUNCTION IN ARCTOMETATARSALIANS

The morphometric and observational resolutions of this study uncover possible variance in function of theropod metatarsi, but the following hypotheses remain tentative in the absence of detailed biomechanical analysis. Most, however, hold substantial promise for more extensive treatment. We begin with the third metatarsal of tyrannosaurids and other arctometatarsalians.

The proximally extensive phalangeal articular surface (in anterior view) of tyrannosaurids indicates potential for more extensive dorsiflexion of the proximal phalanx than for other examined taxa of any size. While this morphology stands out in the context of this limited study, it would be inappropriate to offer hypotheses of functional significance without more detailed analysis.

Generally, proximal and plantar constriction and relative gracility set the arctometatarsalian MT III apart from that of other theropods. The wedge and buttress morphology noted by Holtz (1994, 1995) occurs in all arctometatarsalian forms and is consistent with long axis transfer of ground-reaction forces to the outer metatarsals (Holtz, 1995). It is unclear how the length of the laterally constricted anteroproximal face of the metatarsal (quite short in *Elmisaurus*

and very long in *Troodon*) would affect the energy transfer model (Holtz, 1995). However, other differences of morphological detail may indicate diversity of function in arctometatarsalians.

Specifically, the degree of plantar constriction and the form of proximal intermetatarsal articulations suggest differences in function. The MT III of *Elmisaurus* does not display distal plantar constriction, while the others do. Tyrannosaurids, ornithomimids, and troodontids probably relied upon ligaments to prevent the distal, triangular portion of the third metatarsal from being dislodged anteriorly during footfalls. As Wilson & Currie (1985) note, proximal snap ligaments would have prevented undue posterior rotation of the proximally triangular MT III (with its apex towards the anterior surface) in troodontids. This function may have been present in ornithomimids as well. In contrast, the hook-shaped proximal articulations in tyrannosaurids would have constrained movement, preventing posterior rotation of the proximal part of MT III. Rugosity on adult tyrannosaurid and troodontid metatarsals indicates strong distal ligaments that would have damped anterior rotation of MT III in this region and perhaps unified the foot under high energy footfalls (Snively & Russell, 2002, 2003). Scaling of ligament cross section in arctometatarsalians has yet to be investigated, and it is unclear over what size range these dynamics would occur.

Intermetatarsal ligament scaling and function in alvarezsaurids are equally intriguing. Distal ligaments would be crucial for metatarsal function in the Asian alvarezsaurids *Mononykus olecranus* (Perle *et al.*, 1994; Chiappe, 1997), *Parvicursor remotus* (Karhu & Rautian, 1996), and *Shuvuuia deserti* (Chiappe *et al.*, 2002). Although MT III in these taxa shows typical arctometatarsalian proximal and plantar constriction, the element is restricted to the distal portion of the metatarsus. Because there are no proximal articulations to hold MT III in place, distal ligaments undoubtedly suspended the element (and its associated phalanges) from MT II and IV. The fairly small adult body sizes of these alvarezsaurids may indicate a size threshold above which this arrangement was untenable.

Metatarsal function in other theropods

The most broadly applicable hypothesis is that complex rotation of MT III did not occur in theropods whose metatarsals lacked a distal plantar angulation (where MT III is triangular in cross section and MT II and IV converge towards III's plantar centreline: Fig. 4B, C). Distally, the facing surfaces of their metatarsals were parasagittally orientated and often divergent from each other. If ligaments were present, they would have resisted anteroposterior shear and lateral or medial displacement of the outer metatarsals, but the bones would not be free to move towards the plantar midline as in arctometatarsalian forms. Because most of these taxa lack correlates for distal intermetatarsal ligaments (Snively & Russell, 2003), the moment arm of ligaments holding the metatarsals together was presumably shorter (R. M. Alexander, pers. comm., 1999). The intermetatarsal articulations were probably not as strong overall as they were in arctometatarsalians.

Generally, taxa with an extensive anteroposterior expansion of MT III (for example tyrannosaurids, *Deinonychus*, *Ornitholestes*, and carnosaurs: Table 1) probably had stronger metatarsal articulations in this region than did other taxa. This morphology increased ligament cross section and prevented proximal anteroposterior displacement of MT III.

Peculiarities of MT III morphology evoke more specific hypotheses for several taxa. These hypotheses largely trace the succession of descriptions presented above. Taxa with particularly noteworthy features are discussed, in comparison with tyrannosaurids and other forms.

1. Oviraptorosauria: *Elmisaurus* sp. MT III of this specimen shows proximal constriction on its anterior surface, but plantar constriction is restricted to the distal portion of the metatarsal. As in other caenagnathids (Currie & Russell, 1988), the metatarsals are also fused proximally. Compressive energy would transfer from the distal third metatarsal to the proximal ankylosis of the bones. The energy would therefore not be transmitted by ligaments to the astragalar condyles, as was likely the case in tyrannosaurids, ornithomimids, and troodontids (Holtz, 1995).

2. *Deinonychus antirrhopus*. MT III of *Deinonychus* displays a slight plantar angulation on its medial surface and a distally extensive articular facet for MT II. Neither condition matches the degree of angulation or distal facet area found in arctometatarsalians. However, these morphologies probably correlate with a strong MT II–III articulation in life. *Deinonychus* has a very large, trenchant ungual phalanx on digit II. The strong intermetatarsal articulation would have effectively resisted forces when the animal employed this weapon during predation (Ostrom, 1969).

3. Carnosauria. Unlike in the *Allosaurus* specimens, the MT III of *Sinraptor dongi* slants medially in cross section along its articular surface with MT II. As with *Deinonychus*, there is also a more extensive distal articular facet with MT II. This indicates that the MT II–III articulation was potentially stronger in *Sinraptor* than in *Allosaurus*. Interest-

ingly, MT III of an unnamed giant South American carnosaur (Carcharodontosauridae; P. J. Currie: pers. comm., 2000) reveals a discrete area of distal rugosity on the distal articular surface with MT II (Fig. 8D). MT II of this specimen is unavailable, so it cannot be determined if it bears a rugosity corresponding to that on MT III. However, if the roughened surface on MT III is a ligament scar and not a pathology, these morphologies indicate a diversity of MT II–III articulation mechanisms and strength among large carnosaurs.

The functional implications of this diversity are unclear. *Sinraptor* and large *Allosaurus* specimens were of similar mass (Paul, 1988; 1997), while the carcharodontosaurid was much larger (P. J. Currie: pers. comm., 2000). Metatarsus articulation strength may have correlated with size and/or activity level in carnosaurs, but these hypotheses have yet to be tested.

An arctometatarsus occurs in coelurosaurs of a broad range of sizes (Holtz, 1994, 1995), including tyrannosaurids comparable in size to giant carnosaurs. Therefore aspects of their morphology other than size must be considered in examination of the arctometatarsus' biological role. The following section explores the possible phylogenetic and selective ramifications of the arctometatarsus, with the overriding caveat that hypotheses of biological role are difficult to test adequately.

EVOLUTIONARY MORPHOLOGY OF THE ARCTOMETATARSUS IN A SYSTEMATIC CONTEXT

Functions suggested for the arctometatarsus (Wilson & Currie, 1985; Holtz, 1995; Snively & Russell, 2002, 2003) may have imparted performance advantages that helped ensure an animal's selective success. The distribution of the arctometatarsus on a phylogeny allows us to predict the occurrence of associated features, including intermetatarsal ligaments and an elongate metapodium. Additionally, phylogenetic testing can illuminate the evolution of the arctometatarsus' selective utility. The following discussion outlines pathways of possible evolutionary emergence of the arctometatarsus, and relates them to hypotheses of enhanced locomotor performance.

In discussing origin and evolutionary benefit of the structure, we follow the conventions and terminology of Bock (1965, 1989), Gould & Vrba (1982), Liem (1973), Liem & Osse (1975), and Russell (1979a). An aptation is a morphology or behaviour with current selective utility. It can be a structure refined through selection to impart benefit in its current and sometimes original role (adaptation) or a structure co-opted for a new selective benefit (exaptation: Gould & Vrba, 1981). Aptations can therefore arise neomorphically as

adaptations or exaptively from complexes evolving under different selective circumstances (Bock, 1959, 1963, 1965; Russell, 1979b). Key innovations are aptations that allow the exploitation of new adaptive zones (Liem & Osse, 1975; Russell, 1979a, b). A morphological novelty can yield convergence upon a single functional outcome by multiple modifications of the original structure (Russell,1979a). This results in the original shared structure becoming modified for the same function several times along multiple evolutionary pathways (Bock, 1965).

Convergent acquisition of the arctometatarsus in several coelurosaurian taxa indicates that it emerged along multiple evolutionary pathways. Intermetatarsal ligaments (indicated by rugosity on the articular surfaces) would be a necessary precursor to distal ligament expansion that would strengthen the metatarsus (Holtz, 1995; Hutchinson & Padian, 1997; Snively & Russell, 2003). It is hypothesized that these ligaments were the prerequisite key innovation common to dramatic convergences in foot morphology that occurred in coelurosaurs.

The presence or absence of an arctometatarsus and intermetatarsal ligament correlates, as well as indicators of carnivory, serve as character states that can be mapped onto the two well-corroborated theropod phylogenies in Figure 1 (Holtz, 2000, 2001; Clark *et al.*, 2002). These phylogenies summarize the relationships of taxa bearing an arctometatarsus, and reveal the distribution of intermetatarsal ligaments and the arctometatarsus in coelurosaurs and their sister taxa.

WERE PROXIMAL INTERMETATARSAL LIGAMENTS A KEY INNOVATION IN THE ORIGIN OF THE ARCTOMETATARSUS?

The first hypothesis to be tested is that intermetatarsal ligaments were generally distributed in theropods. Deep ligaments like those proposed for the arctometatarsus often occur between carpals and tarsals in tetrapods (Sisson & Grossman, 1953), but extensive deep ligaments are not normally present between metatarsals. Instead, superficial ligaments attach to the dorsal (or anterior) surfaces of the proximal metatarsal heads, and span the transverse gap between the heads (McGregor, 2000). Diagonal ligaments also occur, running distolaterally from the metatarsal heads to the metatarso-phalangeal joint (McGregor, 2000). Metatarsal shafts do not normally conform tightly, except in some cursorial mammals (Coombs, 1978) and proximally in many dinosaurs. Ligaments on the abutting metatarsal surfaces of theropods would be a novel development, and a logical prerequisite to expansive distal ligaments of the arctometatarsus.

Extrapolatory inference (Bryant & Russell, 1992) indicates that ligaments are the connective tissue

elements most parsimoniously concordant with soft tissue correlates on examined metatarsal articular surfaces (Snively & Russell, 2002, 2003). Facet-delineated rugosity indicating ligaments occurs on proximal intermetatarsal articular surfaces of tyrannosaurids, *Deinonychus*, carnosaurs, *Torvosaurus* (Fig. 11), and in examined TMP and CMN specimens of sauropodomorphs, hadrosaurs and ceratopsians. Similar facets also occur in ornithomimids.

Iterative homology between fore and hind limbs provides circumstantial support for the presence of inter-metatarsal ligaments in carnosaurs and coelurosaurs. Theropod metacarpals articulate tightly with one another proximally, much like the proximal portions of the metatarsals. Roughened intermetacarpal articular facets are present in *Deinonychus antirrhopus* (Ostrom, 1969), and complexly interlocking facets occur on metacarpals of *Acrocanthosaurus atokensis* (Currie & Carpenter, 2000). Although the manus and pes of theropods are disjunct functionally (Gatesy & Dial, 1996), developmental correspondence predicts that if osteological indications of intermetatarsal ligaments are present, correlates of intermetacarpal ligaments would not be surprising.

By bracketed phylogenetic inference (Bryant & Russell, 1992; Witmer, 1995), we can deduce the presence of intermetatarsal ligaments in taxa intervening between *Torvosaurus* and tyrannosaurids (Fig. 11) and in Mesozoic theropods primitively. The postulate emerges that proximal ligaments were a precursor to the acquisition of distal ligaments, which would bind the metatarsals where their distal plantar angulation occurs. Osteological correlates in the arctometatarsus indicate a quantized ontogeny for intermetatarsal ligaments, in which strong ligaments developed proximally and distally, but not in the intermediate region. Further testing will reveal whether or not this apparent ligament ontogeny of the arctometatarsus was the default developmental pattern for coelurosaurs, or how often it became expressed or lost in various taxa.

What selective factors contributed to arctometatarsal evolution?

The hypothesis tested here is that the arctometatarsus was an innovation initially involved in locomotor agility. Henderson & Snively (2003) found that allometric scaling maximized relative agility by minimizing rotational inertia (RI) in tyrannosaurids and other large theropods. RI of a 10 tonne *Tyrannosaurus rex* FMNH PR2081 was computed to be 36% that expected had it retained the same proportions as small theropods (Henderson & Snively, 2003). Ornithomimids and some tyrannosaurids had proportionally low rotational inertias relative to limb muscle mass (E. Sniv-

ely & D. Henderson, unpubl. data). This suggests that the animals imparted higher angular accelerations to their bodies than similarly sized theropods. Biomechanical analysis indicates that the arctometatarsus augmented this agility, at least in tyrannosaurids (Snively & Russell, 2002, 2003), by efficiently channelling torsional forces and preventing splay of the foot. In addition to strengthening the foot for rapid linear locomotion (Holtz, 1995), the arctometatarsus probably enhanced manoeuvrability as well.

Modern animals employ agility in order to procure prey or to escape predators, and during intraspecific combat. Potential modern behavioural analogues suggest parallel hypotheses of biological role for theropods. The long legs of theropods have been considered adaptations enhancing predatory behaviour (Currie, 1997, 2000) and with equal validity as an adaptation associated with increases in home range size (Carrano, 1999).

Although observational corroboration is impossible, hypotheses of the biological role of potential agility are testable by falsification. We can falsify the prey capture hypothesis if herbivory was the primary habit of arctometatarsalian forms. The converse hypothesis, that the arctometatarsus enabled these animals to escape predators, is harder to refute. Presumably, young or small adult arctometatarsalians could employ heightened agility to escape larger theropods, whether the arctometatarsalians were carnivorous or not.

Because coelurosaurs and so many successive out-groups display adaptations for carnivory (Currie, 1997), it is reasonable to infer carnivory in the common ancestor of forms with the potential for the arctometatarsus. Carnivory is indisputable in tyrannosaurids (Erickson *et al.*, 1996; Ryan *et al.*, 2001), and healed tooth marks record predatory activity by *T. rex* (Carpenter, 2000; P. Larsson, pers. comm. 2002). Carnivory occurred in troodontids (Ryan *et al.*, 2000), although Holtz, Brinkman & Chandler (2000) present evidence for troodontid omnivory. Phylogenetic correlation of tyrannosaurid and troodontid arctometatarsi with carnivory suggests the morphology was a predatory aptation in these clades. Under Holtz's (2000) phylogenetic hypotheses and the Bayesian inference results of this study, the structure would be considered primarily adapted for predation, with this biological role lost in ornithomimids.

Toothlessness and other factors (Currie, 1997) indicate a shift from a flesh-based diet in ornithomimids, caenagnathids, and alvarezsaurids. Gastroliths associated with skeletons in an ornithomimid bone bed (Kobayashi *et al.*, 1999) provide evidence of their herbivory. This indicates that the ornithomimid arctometatarsus was exapted for the primary function of escape (Holtz, 2001) or evolved neomorphically for this

function (Clark *et al.*, 2002). Caenagnathids and their oviraptorid relatives, while toothless, had raptorial hands similar to those of dromaeosaurids, with acute recurved claws and joints suggestive of grasping ability. Neonate theropod remains have been found in the nest of an oviraptorid (Clark, Norell & Chiappe, 1999). Predation is therefore a possibility in caenagnathids. If so, agility enhanced by the arctometatarsus may have been beneficial in acquiring prey, although the evidence is sparse and indirect.

The foregoing discussion parsimoniously corroborates agility associated with predation as an initial selective impetus for the arctometatarsus. This conclusion rests on accepting the hypothesis of increased agility in arctometatarsalians and upon a secondary extrapolation that carnivorous coelurosaurs were predaceous. While alternatives are conceivable, the link between the arctometatarus and predatory agility is the most probable scenario.

CONCLUSIONS

1. Description and shape analyses indicate that the arctometatarsus is morphologically distinct from other theropod metatarsi but variable in some details of form and thus function between tyrannosaurids, ornithomimids, troodontids, and caenagnathids.
2. Differences between arctometatarsalian morphologies are consistent with homoplasy, revealed by independent character evidence (Sereno, 1999; Holtz, 2000; Clark *et al.*, 2002) and best documented by Holtz (2001). The present study suggests a minimum of four origins. The structure's developmental expression was possible in coelurosaurs but apparently not in other theropod taxa.
3. Proximal intermetatarsal ligaments were probably a prerequisite to the developmental cascade responsible for the arctometatarsus (including the appearance of extensive distal ligaments).
4. If the arctometatarsus enhanced agility, its probable selective benefit was likely related to predatory performance in carnivorous taxa. Biological roles associated with intra- and interspecific competition and escape were probable at various stages in a possessor's life history.

ACKNOWLEDGEMENTS

REFERENCES

Ahlström T. 1996. Sexual dimorphism in medieval human crania studied by three-dimensional thin-plate spline analysis. In: Marcus LF, Corti M, Loy A, Naylor GJP, Slice DE, eds. *Advances in morphometrics. NATO ASI Series*, Vol. 284**.** New York: Plenum Press, 415–421.

Anderson T. 1963. Asymptotic theory for principal component analysis. *Annals of Mathematical Statistics* **34:** 122–148.

Bergmann PJ. 2003. Systematics and biogeography of the gekkonid lizard *Thecodactylus rapicauda*. Unpublished MSc Thesis. The University of Calgary.

Bock WJ. 1959. Preadaptation and multiple evolutionary pathways. *Evolution* **13:** 194–211.

Bock WJ. 1963. The role of preadaptation and adaptation in the evolution of higher levels of organization. *XVI International Congress of Zoology Washington Proceedings* **3:** 297–300.

Bock WJ. 1965. The role of adaptive mechanisms in the origin of higher levels of organization. *Systematic Zoology* **14:** 272–287.

Bock WJ. 1989. Organisms as functional machines: a connectivity explanation. *American Zoologist* **29:** 1119–1132.

Bookstein FL. 1991. *Morphometric tools for landmark data: geometry and biology*. New York: Cambridge University Press.

Bryant HN, Russell AP. 1992. The role of phylogenetic analysis in the inference of unpreserved attributes of extinct taxa. *Philosophical Transactions of the Royal Society of London, Proceedings B* **337:** 405–418.

Burnaby TP. 1966. Growth-invariant discriminant functions and generalized distances. *Biometrics* **22:** 96–110.

Carpenter K. 2000. Evidence of predatory behavior by carnivorous dinosaurs. *Gaia* **15:** 135–144.

Carrano MT. 1999. What, if anything, is a cursor? Categories versus continua for determining locomotor habit in mammals and dinosaurs. *Journal of Zoology, London* **247:** 29–42.

Chiappe LM. 1997. Aves. In: Currie PJ, Padian K, eds. *Encyclopedia of dinosaurs*. San Diego: Academic Press, 32–38.

Chiappe LM, Norell MA, Clark JM. 2002. The Cretaceous,

short-armed Alvarezsauridae: *Mononykus* and its kin. In: Chiappe LM, Witmer LM, eds. *Mesozoic birds: above the heads of dinosaurs*. Berkeley: University of California Press, 87–120.

Chure DJ. 1995. A reassessment of the gigantic theropod *Saurophagus maximus* from the Morrison Formation of Oklahoma, USA. In: Sun A, Wang Y, eds. *Sixth symposium on Mesozoic terrestrial ecosystems short papers*. Bejing: China Ocean Press, 103–106.

Clark JM, Norell MA, Chiappe LM. 1999. An oviraptorid skeleton from the Late Cretaceous of Ukhaa Tolgod, Mongolia, preserved in an avian-like brooding position over an oviraptorid nest. *American Museum Novitates* **3265:** 1–36.

Clark JM, Norell MA, Makovicky PJ. 2002. Cladistic approaches to the relationships of birds to other theropod dinosaurs. In: Chiappe LM, Witmer LM, eds. *Mesozoic birds: above the heads of dinosaurs*. Berkeley: University of California Press, 31–61.

Cock AG. 1966. Genetical aspects of metrical growth and form in animals. *Quarterly Review of Biology* **41:** 131–190.

Coombs WP Jr. 1978. Theoretical aspects of cursorial adaptations in dinosaurs. *Quarterly Review of Biology* **53:** 393–418.

Currie PJ. 1997. Theropoda. In: Currie PJ, Padian K, eds. *Encyclopedia of dinosaurs*. San Diego: Academic Press, 731–737.

Currie PJ. 2000. Possible evidence of gregarious behavior in tyrannosaurids. *Gaia* **15:** 271–277.

Currie PJ, Carpenter K. 2000. A new specimen of *Acrocanthosaurus atokensis* (Theropoda, Dinosauria) from the Lower Cretaceous Antlers Formation (Lower Cretaceous, Aptian) of Oklahoma, USA. *Geodiversitas* **22:** 207–236.

Currie PJ, Russell DA. 1988. Osteology and relationships of *Chirostenotes pergracilis*. *Canadian Journal of Earth Sciences* **25:** 972–986.

Erickson GM, Van Kirk SD, Su J, Levenston ME, Caler WE, Carter DR. 1996. Bite-force estimation for *Tyrannosaurus rex* from tooth-marked bones. *Nature* **382:** 706–708.

Felsenstein J. 1981. Evolutionary trees from DNA sequences: a maximum likelihood approach. *Journal of Molecular Evolution* **17:** 368–376.

Gatesy SM, Dial KP. 1996. Locomotor modules and the evolution of avian flight. *Evolution* **50:** 331–340.

Gauthier JA. 1986. Saurischian monophyly and the origin of birds. In: Padian K, ed. *The origin of birds and the evolution of flight*. San Francisco: California Academy of Sciences, 1–55.

Gould SJ, Vrba ES. 1982. Exaptation: a missing term in the science of form. *Paleobiology* **8:** 4–15.

Grande L, Bemis WE. 1998. A comprehensive phylogenetic study of amiid fishes (Amiidae) based on comparative skeletal anatomy. An empirical search for interconnected patterns of natural history. Memoirs of the Society of Vertebrate Paleontology. *Journal of Vertebrate Paleontology* **18** *(Suppl. to 1)*: I–x + 690 pp.

Green PJ. 1995. Reversible jump Markov chain Monte Carlo computation and Bayesian model determination. *Biometrika* **82:** 711–732.

Henderson DM. 1999. Estimating the masses and centers of mass of extinct animals by 3-D mathematical slicing. *Paleobiology* **25:** 88–106.

Henderson DM, Snively E. 2003. *Tyrannosaurus* en pointe: Allometry minimized rotational inertia of large carnivorous dinosaurs. *Proceedings of the Royal Society B., Biology Letters* **271:** S57–S60.

Holtz TR Jr. 1994. The phylogenetic position of the Tyrannosauridae: Implications for theropod systematics. *Journal of Paleontology* **68:** 1100–1117.

Holtz TR Jr. 1995. The arctometatarsalian pes, an unusual structure of the metatarsus of Cretaceous Theropoda (Dinosauria: Saurischia). *Journal of Vertebrate Paleontology* **14:** 480–519.

Holtz TR Jr. 2000. A new phylogeny of the carnivorous dinosaurs. *Gaia* **15:** 5–61.

Holtz TR Jr. 2001. Arctometatarsalia revisited: the problem of homoplasy in reconstructing theropod phylogeny. In: Gauthier J, Gall LF, eds. New perspectives on the origin and early evolution of birds: *Proceedings of the international symposium in honor of John H. Ostrom*. New Haven: Peabody Museum of Natural History, Yale University, 99–121.

Holtz TR Jr, Brinkman DL, Chandler CL. 2000. Denticle morphometrics and a possibly omnivorous feeding habit for the theropod dinosaur *Troodon*. *Gaia* **15:** 159–166.

Huelsenbeck JP, Ronquist F. 2003. *MrBayes 3.0: Bayesian inference of phylogeny*. Computer program available at http://morphbank.ebc.uu.se/mrbayes/

Huelsenbeck JP, Ronquist F, Nielsen R, Bollback JP. 2001. Bayesian inference of phylogeny and its impact on evolutionary biology. *Science* **294:** 2310–2314.

Hutchinson JR, Padian K. 1997. Arctometatarsalia. In: Currie PJ, Padian K, eds. *Encyclopedia of dinosaurs*. San Diego: Academic Press, 24–27.

Janensch W. 1925. Die Coelurosaurier und Theropodea der Tendaguru-Schichen Deutch-Ostafricas. *Paleontographica (supplement)* **7:** 1–99.

Jasinoski SJ. 2003. Evolutionary morphology of the theropod scapulacoracoid. Unpublished MSc Thesis. The University of Calgary.

Jolicoeur P. 1963a. The degree of generality of robustness in *Martes americana*. *Growth* **27:** 1–27.

Jolicoeur P. 1963b. The multivariate generalization of the allometry equation. *Biometrics* **19:** 497–499.

Jungers WL, Falsetti AB, Wall CE. 1995. Shape, relative size, and size-adjustment in morphometrics. *Yearbook of Physical Anthropology* **38:** 137–161.

Karhu AA, Rautian AS. 1996. A new family of Maniraptora (Dinosauria: Saurischia) from the Late Cretaceous of Mongolia. *Paleontologicheskii Zhurnal* **30:** 583–592.

Kemp TS. 1999. *Fossils and evolution*. Oxford: Oxford University Press.

Kerfoot WC, Kluge AG. 1971. Impact of the lognormal distribution on studies of phenotypic variation and evolutionary rates. *Systematic Zoology* **20:** 459–464.

Klingenberg CP. 1996. Multivariate allometry. In: Marcus LF, Corti M, Loy A, Taylor GJP, Slice DE, eds. NATO ASI

Series. *Advances in Morphometrics, Series A, Life Sciences* 284: 23–49.

Kobayashi Y, Lu J-C, Dong Z-M, Barsbold R, Azuma Y, Tomida Y. 1999. Herbivorous diet in an ornithomimid dinosaur. *Nature* **402:** 480–481.

Kurzanov SM. 1983. An unusual theropods from the Upper Cretaceous of Mongolia. Iskorayenyye pozvonochneyye Mongolii (Fossil Vertebrates of Mongolia). *Trudy Sovmestnay Sovetsko-Mongolskay Paleontologiyeskay Ekspeditsiy* **15:** 39–50.

Larget B, Simon D. 1999. Markov chain Monte Carlo algorithms for the Bayesian analysis of phylogenetic trees. *Molecular Biology and Evolution* **16:** 750–759.

Lauder GV. 1995. On the inference of function from structure. In: Thomason JJ, ed. *Functional morphology in vertebrate paleontology*. Cambridge: Cambridge University Press, 1–18.

Leamy L, Bradley D. 1982. Static and growth allometry of morphometric traits in random bred house mice. *Evolution* **36:** 1200–1212.

Lewis PO. 2001. A likelihood approach to estimating phylogeny from discrete morphological character data. *Systematic Biology* **50:** 913–925.

Liem KF. 1973. Evolutionary strategies and morphological innovations: cichlid pharyngeal jaws. *Systematic Zoology* **22:** 425–441.

Liem KF, Osse JWM. 1975. Biological versatility, evolution, and food resource exploitation in African cichlid fishes. *American Zoologist* **15:** 427–454.

Maddison W, Maddison D. 2003. *Mesquite 0.993d42.* Computer program available at http://www.mesquiteproject.org/

Marcus L. 1990. Traditional morphometrics. In: Rohlf FJ, Bookstein FL, eds. *Proceedings of the Michigan morphometrics workshop*. Special Publication no. 2, The University of Michigan Museum of Zoology, 77–122.

Mau B, Newton M, Larget B. 1999. Bayesian phylogenetic inference via Markov chain Monte Carlo methods. *Biometrics* **55:** 1–12.

McGregor LD. 2000. Locomotor morphology of *Anolis*: comparative investigations of the design and function of the subdigital adhesive system. Unpublished MSc Thesis. The University of Calgary.

McKinney ML. 1990. Trends in body-size evolution. In: McNamara KJ, ed. *Evolutionary trends*. Tucson: The University of Arizona Press.

McKinney ML, McNamara KJ. 1991. *Heterochrony. The evolution of ontogeny*. New York: Plenum Press.

Morrison DF. 1976. *Multivariate statistical methods*, 2nd edn. Montreal: McGraw-Hill.

Novas FE. 1994. New information on the systematics and postcranial skeleton of *Herrerasaurus ischigualastensis* (Theropoda: Herrerasauridae) from the Ischigualasto Formation (Upper Triassic) of Argentina. *Journal of Vertebrate Paleontology* **13:** 400–423.

Ostrom JH. 1969. Osteology of *Deinonychus antirrhopus*, an unusual theropod from the Lower Cretaceous of Montana. *Bulletin of the Peabody Museum of Natural History* **30:** 1–165.

Paul GS. 1988. *Predatory dinosaurs of the world*. New York: Simon and Schuster.

Paul GS. 1997. Dinosaur models: the good, the bad, and using them to reconstruct the mass of dinosaurs and other extinct vertebrates. In: Wolberg DL, Stump EL, Rosenberg T, eds. Dinofest International. *Proceedings of a symposium held at Arizona State University*. Philadelphia: The Academy of Natural Sciences, 129–154.

Perle A. 1979. Segnosauridae-A new family of theropods from the Late Cretaceous of Mongolia. *Soviet-Mongolian Paleontological Expedition, Transactions* **8:** 45–55.

Perle A, Chiappe LM, Barsbold R, Clark JM, Norell MA. 1994. Skeletal morphology of *Mononykus olecranus* (Theropoda: Avialae) from the Late Cretaceous of Mongolia. *American Museum Novitates* **3105:** 1–29.

Pimentel RA. 1979. *Morphometrics, the multivariate analysis of biological data*. Dubuque: Kendall/Hunt.

Reig OA. 1963. La presencia de dinosaurios saurisquios en los 'Estrados de Ischigualasto' (Mesotriasico superior) de las Provincias de San Juan y La Rioja (Republica Argentina). *Ameghiniana* **3:** 3–20.

Reyment RA. 1990. Reification of classical multivariate statistical analysis in morphometry. In: Rohlf FJ, Bookstein FJ, eds. *Proceedings of the Michigan morphometrics workshop*. Special Publication no. 2, The University of Michigan Museum of Zoology, 123–144.

Rohlf FJ, Bookstein FL. 1987. A comment on shearing as a method for 'size correction'. *Systematic Zoology* **36:** 356–367.

Russell AP. 1979a. Parallelism and integrated design in the foot structure of gekkonine and diplodactyline geckos. *Copeia* **1979:** 1–21.

Russell AP. 1979b. The origin of parachuting locomotion in gekkonid lizards (Reptilia: Gekkonidae). *Zoological Journal of the Linnean Society* **65:** 233–249.

Ryan MJ, Currie PJ, Gardner JD, Vickaryous MK, Lavigne JM. 2000. Baby hadrosaurid material associated with an unusually high abundance of *Troodon* teeth from the Horseshoe Canyon Formation, Upper Cretaceous, Alberta. *Gaia* **15:** 123–133.

Ryan MJ, Russell AP, Eberth DA, Currie PJ. 2001. The taphonomy of a *Centrosaurus* (Ornithischia, Certopsidae) bone bed from the Dinosaur Park Formation (upper Campanian), Alberta, Canada, with comments on cranial ontogeny. *Palaios*. **16:** 482–506.

Sereno PC. 1999. The evolution of dinosaurs. *Science* **284:** 2137–2147.

Shea BT. 1985. Bivariate and multivariate growth allometry: Statistical and biological considerations. *Journal of Zoology, London* **206:** 367–390.

Sisson S, Grossman JD. 1953. *The anatomy of domestic animals.* Philadelphia: Saunders.

Snively E. 2000. Functional morphology of the tyrannosaurid arctometatarsus. Unpublished MSc Thesis, University of Calgary.

Snively E, Russell AP. 2002. The tyrannosaurid metatarsus: bone strain and inferred ligament function. *Senckenbergiana Lethaea* **81:** 73–80.

Snively E, Russell AP. 2003. A kinematic model of tyranno-

saurid arctometatarsus function (Dinosauria: Theropoda). *Journal of Morphology* **255:** 215–227.

Somers KM. 1986. Multivariate allometry and removal of size with principal component analysis. *Systematic Zoology* **35:** 359–368.

Strauss RE. 1987. On allometry and relative growth in evolutionary studies. *Systematic Zoology* **36:** 72–75.

Swiderski DL. 1994. Morphological evolution of the scapula in tree squirrels, chipmunks, and ground squirrels (Sciuridae): an analysis using thin-plate splines. *Evolution* **47:** 1854–1873.

Tissot BN. 1988. Multivariate analysis. In: McKinney ML, ed. *Heterochrony in evolution. A multidisciplinary approach.* New York: Plenum Press.

Voss RS. 1988. Systematics and ecology of ichthyomyine rodents (Muroidea). *Bulletin of the American Museum of Natural History* **188:** 1–493.

Wilson MC, Currie PJ. 1985. *Stenonychosaurus inequalis* (Saurischia: Theropoda) from the Judith River (Oldman) Formation of Alberta: New findings on metatarsal structure. *Canadian Journal of Earth Sciences* **22:** 1813–1817.

Witmer LM. 1995. The extant phylogenetic bracket and the importance of reconstructing soft tissues in fossils. In: Thomason JJ, ed. *Functional morphology in vertebrate paleontology.* Cambridge: Cambridge University Press, 19–33.

Xu X, Wang X-L, Wu X-C. 1999. A dromaeosaurid dinosaur with a filamentous integument from the Yixian Formation of China. *Nature* **401:** 262–266.

Zar JH. 1984. *Biostatistical analysis*, 2nd edn. Englewood Cliffs, NJ: Prentice Hall.

APPENDIX 1

BACKGROUND TO PRINCIPAL COMPONENT ANALYSIS (PCA)

It is most convenient to compare the simultaneous size-dependent shape variance of several anatomical dimensions in terms of allometry (Jolicoeur, 1963a; Cock, 1966; Pimentel, 1979; Shea, 1985; Strauss, 1987; Voss, 1988; McKinney & McNamara, 1991). The principal component generalization of the allometric equation (Jolicoeur, 1963b) describes multivariate scaling (Jolicoeur, 1963a; Pimentel, 1979; Shea, 1985; Rohlf & Bookstein, 1987; Strauss, 1987; Voss, 1988; McKinney & McNamara, 1991; Jungers, Falsetti & Wall,1995). In PCA of log-transformed data from a single taxonomic group, the first component (the 'size-determined shape vector:' McKinney, 1990) represents the variation incident upon differences in size (Somers, 1986; Tissot, 1988; McKinney, 1990; McKinney & McNamara, 1991). Subsequent components describe shape variation that is not directly associated with size (Tissot, 1988; Marcus, 1990; McKinney, 1990; McKinney & McNamara, 1991).

Because our PCA subsumes all lower-order taxa into Theropoda, we ignore the variance accounted for by phylogeny of the sample and the lack of independence among its members (Klingenberg, 1996). However, it is unlikely that we confound evolutionary and ontogenetic scaling. The small sample size precludes partitioning of low-level phylogenetic variance, but introduces the possibility that idiosyncratic variation of one or more specimens is assigned undue significance in either of the PCAs. Against these caveats, the initial PCA assigned the bulk of the sample variance to three components (Table 3), indicating that most sample variance could not be attributed to multitudinous and dramatic low-level phylogenetic differences. The clustering of most specimens' first and second PC scores (Figs 2, 3), and the amount of nonsize-associated variance explained by PCII and PCIII in the PCA of the isometry-removed data, suggest that any idiosyncratic shape or size variation contributed little to the total sample variance.

METHODS FOR PCA: JUSTIFICATION AND PROCEDURES

Raw measurements were $\log_{10}$-transformed to minimize possible inherent heteroscedasticity (Kerfoot & Kluge, 1971; Zar, 1984; Tissot, 1988), to better approximate the multivariate normal distribution (Pimentel, 1979; Marcus, 1990; of less importance in this case, as we are effectively ordinating our data – Reyment, 1990), and to better approximate the linear PCA model (Jolicoeur, 1963a; Pimentel, 1979; Shea, 1985; Strauss, 1987; Voss, 1988). PCA was performed on a variance-covariance matrix derived from the $\log_{10}$-transformed data. Treating each specimen as a point in an ordination is a legitimate use of PCA, especially in cases such as this, where the groups are not well defined (Marcus, 1990) or represented by single cases.

The seven components of the PCA (PCI–VII) were retained and the loadings standardized (McKinney & McNamara, 1991). PCII–VII were tested for equal length and isotropicity of variance by Bartlett's χ^2 test for sphericity (Morrison, 1976; since the sample sizes are small. Only nonisotropic components were examined further. PCI was interpreted as the size-determined shape vector, while the remainder were examined for evidence of morphological changes not strongly determined by overall size (Tissot, 1988; Marcus, 1990; McKinney & McNamara, 1991; Jungers *et al.*, 1995). We calculated correlations of each variable with each component, and the percent of the total variation of each variable explained by each component (Pimentel, 1979). The first was tested for isometry (defined as being a vector of loadings, all pairwise combinations thereof producing isometric bivariate reduced major axis slope estimates – Klingenberg, 1996) by comparing it to a theoretical 'isometric vector' (Leamy & Bradley, 1982; Voss, 1988). The individual loadings of the isometric vector are computed as $1/\sqrt{p_i}$,

where p_i = number of variables in the analysis (Jolicoeur, 1963b); in the case of the present analyses, all loadings on the theoretical isometric vector = $1/\sqrt{7} = 0.377964$. This was compared to PCI by means of Anderson's χ^2 approximation (Anderson, 1963; Pimentel, 1979). An individual variable loading of the first component that approximates the value of the isometric loading demonstrates isometry for its variable [i.e. equality of relative growth rates (Jolicoeur, 1963a)] relative to an overall measure of size (i.e. the weighted geometric mean of all variables – Klingenberg, 1996). Variable loadings considerably greater than the isometric loading indicate positive allometry, and variable loadings well below the isometric loading indicate negative allometry, for their respective variables (Voss, 1988).

The second and third components from the initial PCA were tested for equal length and isotropicity of variation by Bartlett's χ^2 test for sphericity (Morrison, 1976), since the sample sizes are small. The findings of this test were taken into account in interpretations of the second and third components. We consequently used the theoretical isometric vector with the Burnaby method for size-correction (Burnaby, 1966; Rohlf & Bookstein, 1987; Marcus, 1990) to generate a modified data matrix from which all of the variance explained by geometric similarity in shape was removed. A means-centred data matrix was not required, since there was only one group of cases. This modified data matrix was then used to derive a second set of principal components and ancillary statistics, which were examined to determine within-group differences among the MT IIIs not attributable to size associated with geometric similarity. The Bartlett's χ^2 test for sphericity was likewise applied to the principal components arising from this second PCA in order to determine the number of components which could be meaningfully interpreted.

APPENDIX 2

Measurements (mm) and principal component scores of theropod third metatarsals. LTOTAL, total length; PW, proximal width; W25%, width at 25% of LTOTAL from proximal end. W50%, width at 50% of LTOTAL; W75%, width at 75% of LTOTAL from proximal end; DW, distal width; HPAS, proximo-distal extent (height) of phalangeal articular surface in anterior view. *Segnosaurus*: Perle (1979). *Ornitholestes*: Paul (1988). *Allosaurus maximus*: Chure (1995). *Elaphrosaurus*: Janensch (1925). *Herrerasaurus*: Reig (1963)

Taxon	Specimen number W50% PCI	LTOTAL W75% PCII	WPROX WDIST PCIII	W25% HPAS
Ornithomimidae	TMP 87.54.1 14.3 −0.4200293	304.3 28.5 0.2365663	17.3 32.1 −0.0633047	9.1 18.5
Troodon formosus	MOR 12.1 −0.3369449	433.2 28.0 0.619731	14.6 50.5 −0.0993321	5.8 34.6
Troodon formosus	TMP 91.26.575 6.3 −0.8778112	257.9 17.8 0.4749723	10.0 28.3 −0.1414081	5.1 18.4
Albertosaurus sarcophagus	AMNH 5432 26.9 0.606663	585.0 62.7 0.3306354	39.3 92.6 −0.0428058	27.0 62.0
Albertosaurus sarcophagus	TMP 86.64.1 19.7 0.2456245	484.4 54.7 0.3415919	23.8 73.6 0.0318129	20.0 37.2
Gorgosaurus libratus	TMP 81.10.1 29.6 0.578768	544.2 64.0 0.3048399	34.3 90.0 0.0301007	27.3 58.2
Tyrannosaurus rex	LACM 7244/23844 52.8 0.968426	605.0 96.5 0.2980288	46.8 131.5 0.1011046	33.2 82.6
Tyrannosaurus rex	MOR 555 56.5 1.121266	647.8 105.8 0.267356	65.3 148.2 0.0192932	37.5 90.6
Tyrannosaurus rex	FMNH PV 2081 50.2 1.1430502	655.6 108.7 0.209041	78.0 147.1 −0.0491865	43.0 79.6
Tarbosaurus bataar	PIN 552–1 22.6 0.6779677	571.0 88.3 0.3469923	37.3 106.5 0.0105706	33.7 58.9
Elmisaurus sp.	TMP/PJC 8.7 −0.8892942	166.1 13.9 0.1427501	13.4 24.9 −0.1653533	6.7 13.6
Chirostenotes pergracilis	NMC 8538 15.0 −0.7333694	230.2 22.5 0.2259328	6.5 22.5 0.2772402	9.5 17.3
Rinchenia mongoliensis	GI 100/42 17.0 −0.7053687	180.0 19.6 0.0237041	9.3 21.3 0.1821319	11.2 14.9
Ingenia yanshini	GI 100/34 8.8 −1.3484338	75.0 9.4 −0.2199639	7.7 11.4 0.0401064	8.2 7.5
Ingenia yanshini	GI 100/32 15.0 −0.7967007	129.4 17.4 −0.0641503	9.2 22.4 0.1681986	11.6 12.8
Deinonychus antirrhopus	MOR 793 11.9 −1.0014499	132.6 13.1 −0.1120287	8.5 19.1 0.099382	10.5 8.6
Deinonychus antirrhopus	YPM 5205 15.0 −0.7692143	145.4 18.0 −0.1458697	9.9 23.6 0.1585397	14.2 9.4

APPENDIX 2 *Continued*

Taxon	Specimen number W50% PCI	LTOTAL W75% PCII	WPROX WDIST PCIII	W25% HPAS
Bambiraptor feinbergi	AMNH 30556 5.1 −1.8286753	76.2 6.2 −0.0317622	4.2 8.2 0.0193373	4.2 5.7
Segnosaurus ghalbinensis	GI SPS 100182 51.0 0.7291561	284.4 52.0 −0.3739572	73.6 95.0 −0.0460691	64.9 26.3
Ornitholestes hermani	AMNH 619 7.0 −1.3616157	112.4 7.9 −0.0453385	7.2 11.2 −0.0372921	7.4 9.6
Sinosauropteryx prima	MV91 127587 6.7 −1.6707526	57.0 6.5 −0.3362013	7.3 8.0 −0.0572452	6.5 4.7
Coelurosauria	NAMAL 13.5 −0.6142761	216.6 14.3 0.0229432	15.0 24.9 −0.0652885	12.5 17.6
Fukuiraptor kitadaniensis	FPMN 9712224 23.8 0.0052948	296.5 26.8 0.0115059	24.4 44.7 0.0058124	23.5 29.7
Sinraptor dongi	IVPP 10600 55.7 0.7202153	416.0 57.1 −0.2786048	69.2 76.4 −0.0318138	54.0 25.8
Allosaurus fragilis	MOR 693 49.2 0.7764009	341.8 48.5 −0.2669379	96.4 74.2 −0.1813149	53.1 41.5
Allosaurus fragilis (right)	ROM 5091 57.4 0.8124952	378.7 59.9 −0.2161356	67.8 80.0 0.0032102	58.3 41.3
Allosaurus fragilis (left)	ROM 5091 68.7 0.993843	373.0 70.8 −0.202174	81.2 97.0 0.0069512	63.6 54.2
Allosaurus jimmadseni	DINO 11541 44.0 0.5266594	320.0 45.5 −0.1233616	53.0 76.0 −0.0460868	34.0 34.0
Allosaurus maximus	OMNH 01708 74.9 1.1856372	462.7 89.4 −0.1438707	96.9 127.8 −0.01049	69.1 60.3
Carcharodontosauridae	PVPH 108–31 71.0 1.0749872	450.0 74.4 −0.1121854	69.7 112.4 0.0747103	70.0 66.3
cf. Tetanurae	BYU 7253647 53.2 0.7455451	405.4 63.0 −0.2187465	64.1 93.0 −0.0051746	51.5 26.8
Torvosaurus tanneri	BYU 7255277 70.2 0.9538025	351.2 70.1 −0.1521572	77.6 103.2 0.0048173	50.6 54.7
Torvosaurus tanneri	BYU 7255280 77.6 1.0172349	362.1 73.2 −0.2959451	76.9 106.8 0.0726465	77.0 42.6
Elaphrosaurus bambergi	HMN dd 25.4 0.0069038	304.0 28.5 −0.1066687	28.8 37.6 −0.0218317	26.5 22.6
Coelophysis bauri	TMP block 6.4 −1.5189771	106.0 7.0 −0.1915045	9.3 7.9 −0.1695912	6.5 5.8
Herrerasaurus ischigualestensis	PVL 2566 25.2 −0.0170276	224.6 26.4 −0.219027	33.4 45.3 −0.0723773	26.6 18.0